Bovine herpesvirus 4-based vector delivering a hybrid rat/human HER-2 oncoantigen efficiently protects mice from autochthonous Her-2+ mammary cancer.

In Oncoimmunology, 2015

***DOI:** 10.1080/2162402X.2015.1082705*

Bovine herpesvirus 4-based vector delivering a hybrid rat/human HER-2 oncoantigen efficiently protects mice from autochthonous Her-2$^+$ mammary cancer.

Sarah Jacca[aΔ], Valeria Rolih[bΔ], Elena Quaglino[bΔ], Valentina Franceschi[a], Giulia Tebaldi[a], Elisabetta Bolli[b], Alfonso Rosamilia[a], Simone Ottonello[c], Federica Cavallo[b]* and Gaetano Donofrio[a]*

[a]*Department of Medical-Veterinary Science, University of Parma, Parma, Italy.* [b]*Department of Molecular Biotechnology and Health Sciences, Molecular Biotechnology Center, University of Torino, Torino, Italy.* [c]*Department of Life Sciences, Biochemistry and Molecular Biology Unit, University of Parma, Parma, Italy.*

[Δ]These authors equally contributed to this work

Corresponding authors:

*Gaetano Donofrio

Departement of Medical Veterinary-Science

Via del Taglio 8, 43126 Parma, Italy

Tel.: 00390521902677

E-Mail: gaetano.donofrio@unipr.it

*Federica Cavallo

Department of Molecular Biotechnology and Health Sciences

Molecular Biotechnology Center

Via Nizza 52, 10126 Torino, Italy

Phone: 0039 011 670 6457/6458

Federica.cavallo@unito.it

ABSTRACT

The HER-2 oncogene is a major target for the immunotherapy of breast cancer. Following up to the therapeutic success achieved with Her-2-targeting monoclonal antibodies, immune-prophylactic approaches directed against Her-2 have also been investigated taking into account, and trying to overcome, Her-2 self-tolerance. Perhaps due to safety (and efficacy) concerns, the least explored anti-Her-2 active immunization strategy so far has been the one relying on viral-vectored vaccine formulations. Taking advantage of the favorable properties of bovine herpesvirus 4 (BoHV-4) in terms of safety and ease of manipulation as well as its previously documented ability to transduce and confer immunogenicity to heterologous antigens, we tested the ability of different recombinant HER-2-BoHV-4 immunogens to break tolerance and elicit a protective, anti-mammary tumor antibody response in HER-2 transgenic BALB-neuT mice. All the tested constructs expressed the HER-2 transgenes at high levels and elicited significant cellular immune responses in BALB/c mice upon administration via either DNA vaccination or viral infection. In BALB-neuT mice, instead, only the viral construct expressing the membrane-bound chimeric form of Her-2 protein (BoHV-4-RHuT-gD) elicited a humoral immune response that was more intense and earlier-appearing than that induced by DNA vaccination. In keeping with this observation, two administrations of BoHV-4-RHuT-gD effectively protected BALB-neuT mice from tumor formation, with 50% of vaccinated animals tumor-free after 30 weeks from immunization compared to 100% of animals exhibiting at least one palpable tumor in the case of animals vaccinated with the other BoHV-4-HER-2 constructs.

Keywords: Her-2 oncogene, HER-2 immunogens, BoHV-4-based vector, recombinant BoHV-4s, BALB-neuT mice, vaccination.

Abbreviations: HER-2, epidermal growth factor receptor 2; TK, tyrosine kinase; ATP, adenosine triphosphate; BoHV-4, bovine herpesvirus 4; HSV-1, herpes simplex virus 1; IgG, immunoglobulin G; Fc, crystallizable fragment; IFN-γ, interferon gamma; HEK, human embryo kidney; BEK, bovine embryo kidney; gD, glycoprotein G; DMEM, Dulbecco's modified eagle medium; EMEM, Eagle's minimal essential medium; TCID50, tissue culture infectious dose 50; M.O.I., multiplicity of infection; BSA, bovine serum albumin; ELISPOT, enzyme linked immune-spot; PBS, phosphate buffer saline; BAC, bacteria artificial chromosome; RPMI, Roswell Park Memorial Institute medium; PCR, polymerase chain reaction; PEI, polyethylenimine; FBS, fetal bovine serum; LB, Luria Bertani's medium; CPE, cytopathic effect; CFSE, carboxyfluorescein-diacetate-succinimidyl ester. SEM, standard error mean; SFU, spot forming units; SPC, spot-forming cells.

INTRODUCTION

Despite the significant therapeutic improvements achieved in the last decades, breast cancer remains the most important, women-affecting, solid neoplasm worldwide [1]. Overexpression of the epidermal growth factor receptor 2 (HER-2) oncogene - mainly due to gene amplification-based mechanisms [2, 3] occurs in ~15-25% breast cancers, where it has been consistently associated with metastatization propensity, poor prognosis and reduced survival [4].

Her-2 is a four transmembrane domain tyrosine kinase (TK) receptor. Although it is structurally and functionally well characterized, its specific ligand is still unknown. Her-2 homo/hetero dimerization induces TK domain phosphorylation, thus triggering the activation of multiple signal transduction pathways [5-7]. Among these pathways, those centered on the Ras/Raf mitogen-activated protein kinase and the phosphatidil-inositole-3-kinase are the best characterized. Their deregulated activation is causally involved in cancerous phenotype development and results in altered cellular growth/division, differentiation and adhesion properties [5-7]. For these reasons, Her-2 and its associated pathways are major clinical therapeutic targets. At present, two main classes of molecules are employed in the clinic to target Her-2. The first is represented by humanized monoclonal antibodies (Trastuzumab and Pertuzumab), that by targeting the extracellular portion of the receptor, interfere with Her-2 dimerization thus inducing receptor endocytosis and degradation [8, 9]. Importantly, these antibodies can also activate antibody- and complement-mediated cellular cytotoxicity [10]. The second class of therapeutics is composed of synthetic small-molecules that interact with the ATP-binding site of the intracellular TK domain of Her-2 and block receptor phosphorylation/activation, thus preventing downstream signaling events [1, 11]. Of note, Trastuzumab and Her-2 TK domain inhibitors have been shown to act synergistically thus paving the way to their combined therapeutic use also in association with traditional endocrine, chemo and radiation therapies [1].

Prompted by the effectiveness of passive immunization relying on anti-Her-2 antibodies, immune-prophylactic, active immunization approaches directed against Her-2 have also been extensively explored in preclinical models of mammary cancer [12, 13]. However, since Her-2 is a self-tolerated antigen

(Ambrosino *et al.*, 2006), a major hurdle for these approaches has been the breaking of central and peripheral tolerance [14-17]. Several ways to overcome this problem have been developed [18-20], including vaccination with hybrid DNA constructs coding for chimeric rat/human Her-2 proteins [21-23].

A very little explored, but potentially promising tolerance breaking/immunization strategy relies on the use of viral-vectored vaccine formulations. In fact, viral vectors can deliver the antigen directly into host cells, thus leading to high-level transgene cellular expression. Key properties of an effective, and potentially translatable, viral vector are safety, the ability to properly present the expressed antigen to the immune system and to remain within host cells long enough to stimulate an effective response. A viral vector apparently meeting these criteria, including ease of manipulation (with the possibility to insert up to 30 kb of foreign DNA) and the ability to confer strong immunogenicity to heterologous antigens, is bovine herpesvirus 4 (BoHV-4). Cattle is the natural host of this virus, but BoHV-4 isolates have been retrieved from other animal species as well. *In vitro*, BoHV-4 is able to replicate in primary cultures and cell lines from a variety of animal species [24-30]. Experimental infection of many non-natural hosts [mice [28], rats [31], rabbits [27], sheep [25], swine [32] and goats [30] as well as *ex vivo* tissue explants from non-human primates has been documented (personal communication), suggesting that BoHV-4 is most likely also competent for human cell transduction. In infected mice, BoHV-4 behaves as a replication-incompetent virus [33] that preferentially localizes to cells of the monocyte/macrophage lineage [34]. At variance with other gamma-herpesviruses, no evidence for growth-transformation, nor any virus-associated pathology has been reported for BoHV-4 so far. In fact, recombinant BoHV-4s expressing immune-dominant antigens from different pathogens have been successfully employed to immunize genetically modified mice without any detrimental effect, overt clinical sign or pathology correlated to viral vector inoculation [28]. Furthermore, a BoHV-4-based vector armed with a Herpes Simplex virus-1 thymidine kinase (HSV-1-TK) gene displayed enhanced oncolytic properties in immune-competent orthotopic syngenic mouse and rat glioma models [29].

In view of all these favorable properties, and good potential for clinical translation, we set out to test BoHV-4 as a HER-2 expression carrier and novel immuno-prophylactic agent against Her-2^+ mammary

115 cancer. Since vaccine delivery and cellular localization of vaccine-encoded antigens are key factors in
116 modulating the induced immune responses, we assembled different recombinant HER-2-BoHV-4 viral
117 vectors and tested their immunogenicity as well as cancer prevention capacity. The recombinant vector
118 expressing the membrane-bound form of a hybrid, rat-human Her-2 antigen was found to be the only
119 one capable of eliciting high anti-Her-2 antibody titers in immune-tolerant, rat HER2 transgenic
120 (BALB-neuT) mice and to afford strong protection against autochthonous Her-2^{+} mammary cancer
121 development in these animals.
122
123

RESULTS

Design and expression of different Her-2 chimeric proteins

Before generating BoHV-4-based vectors expressing specific portions of HER-2 oncogene, three optimized ORFs coding for different HER-2 derived chimeric fragments were customized taking into account antigen subcellular localization and recognition by the immune system. RHuT-gD, a cell surface associated form, was assembled by fusing the N-terminal 1-390 aminoacids (aa.) region of rat HER-2 with 299 amino acids (residues 301-691) derived from the C-terminal region of human HER-2 and gD106, a 33 peptide tag derived from bovine herpesvirus-1 glycoprotein D [35] **(see Supplementary Fig. 1)**. RRT-gD, a secreted form lacking the transmembrane domain, was constructed by fusing the N-terminal 1-390 amino acids region of rat HER-2 with the gD106 tag peptide **(Supplementary Fig. 2)**. An additional secreted form, potentially capable of interacting with Fc receptors and designated RRT-Fc, was generated by substituting the HgD106 region of RHuT-gD with a stretch of 240 amino acids derived from the C-terminus of mouse IgG Fc **(**see **Supplementary Fig. 3)**. RHuT-gD, RRT-gD and RRT-Fc were all placed under the transcriptional control of the CMV promoter and the bovine growth hormone polyadenylation signal to obtain the CMV-RHuT-gD, CMV-RRT-gD and CMV-RRT-Fc expression cassettes. The latter cassettes were excised from the plasmid backbone and sub-cloned into the pINT2 shuttle vector containing two BoHV-4 TK flanking sequences [24], in order to generate the targeting vectors pTK-CMV-RHuT-gD-TK (pINT2-RHuT-gD), pTK-CMV-RRT-gD-TK (pINT2-RRT-gD) and pTK-CMV-RRT-Fc-TK (pINT2-RRT-Fc) **(Fig. 1A, B and C)**. The resulting constructs were functionally validated in terms of protein expression by transient transfection into HEK 293T cells and immunoblotting with a monoclonal antibody directed against the gD106 tag peptide. All three chimeric proteins were well expressed in transfected cells **(Fig. 1D, E and F)** and, as expected, RRT-gD and RRT-Fc were found to be secreted **(data not shown)**.

Immunogenicity profiling of the different HER-2 constructs delivered to syngeneic mice by DNA vaccination

Although all three targeting vectors (pINT2-RHuT-gD, pINT2-RRT-gD and pINT2-RRT-Fc) led to high chimeric Her-2 protein levels in HEK 293T cells, we wished to evaluate their immunogenic properties more directly before converting them to the corresponding viral delivery vectors. To this end, three groups of BALB/c mice (6 animals/group) were immunized twice, at two-weeks intervals, with 50 μg of each plasmid and anti-rat Her-2 humoral and cellular immune responses were evaluated two weeks after the second vaccination. A targeting vector, pTK-CMV-A29gD-TK (pINT2-A29-gD), carrying an unrelated antigen from Monkeypoxvirus [36], was administered to a fourth group of mice and served as a negative control. Only mice vaccinated with pINT2-RHuT-gD, the plasmid coding for the membrane-bound form of the antigen, yielded a well-detectable anti-rat-Her-2 antibody response **(Fig. 2A)**. However, as revealed by parallel *in vivo* cytotoxicity assays using lysis of syngeneic splenocytes pulsed with the immune-dominant (H-2^d) rat Her-2 peptide TYVPANASL as readout, all plasmids elicited a specific anti rat-HerR-2 cellular immune response **(Fig. 2B).** Similarly, all plasmids triggered IFN-γ-producing cells upon TYVPANASL peptide re-stimulation in ELISPOT assays **(Fig. 2C)**.

To determine immunogenicity in a mouse model more closely resembling the cancer situation (i.e., HER-2 overexpression), we next evaluated the ability of pINT2-RHuT-gD, pINT2-RRT-gD and pINT2-RRT-Fc to induce anti-rat Her-2 antibodies in BALB-neuT mice [37]. These mice display a central tolerance with deletion of rat Her-2 TYVPANASL peptide-reactive $CD8^+$ T cells [14, 15]. Following vaccination (16-week-old BALB-neuT mice; n=7 per group), only animals receiving the pINT2-RHuT-gD plasmid displayed a significant anti-rat Her-2 humoral immune response **(**see **Supplementary Fig. 4)**. As expected, given the expression of rat-Her-2 in the thymus of newborn BALB-neuT mice [21], these animals failed to mount any *in vivo* cytotoxic response against the TYVPANASL peptide and no IFN-γ was produced by splenocytes derived from vaccinated BALB-neuT mice upon TYVPANASL re-stimulation **(data not shown).**

Despite the unique ability of pINT2-RHuT-gD to elicit anti-rat Her2 antibodies in both mouse strains, all plasmids appeared to be capable to induce cellular immune responses in BALB/c mice. Therefore all three targeting vectors were carried on and used to construct the corresponding recombinant viruses.

Construction of recombinant BoHV-4 viruses containing different HER-2 expression cassettes

The genome molecular clone of a safe BoHV-4 isolate (designated as BoHV-4-A) derived from the milk cell fraction of a clinically healthy cow [26] was used to construct the three recombinant HER2-BoHV-4 vectors (BoHV-4-RHuT-gD, BoHV-4-RRT-gD and BoHV-4-RRT-Fc) plus a control viral vector (BoHV-4-A29-gD) delivering a completely unrelated antigen. To this end, pINT2-RHuT-gD, pINT2-RRT-gD, pINT2-RRT-Fc and the pINT2-A29-gD plasmid vectors were first linearized by a restriction enzyme digestion sparing the BoHV-4 TK flanking regions. Linearized plasmids were then electroporated into SW102 *E. coli* cells containing the artificial chromosome pBAC-BoHV-4-A-KanaGalKΔTK [26, 38, 39] **(Fig. 3A),** in order to generate pBAC-BoHV-4-A-CMV-RHuT-gD-ΔTK, pBAC-BoHV-4-A-CMV-RRT-gD-ΔTK, pBAC-BoHV-4-A-CMV-RRT-Fc-ΔTK **(Fig. 3B)** and pBAC-BoHV-4-A-CMV-A29-gD-ΔTK artificial chromosomes via heat-inducible homologous recombination [40]. The TK locus of the BoHV-4 genome is extremely stable even after repeated passages *in vitro* and *in vivo*, and it can thus be reliably employed to integrate foreign DNA sequences into the BoHV-4 genome without any transgene or viral replication efficiency loss due to recombination [24-30].

Selected SW102 *E. coli* clones carrying pBAC-BoHV-4 recombinants were analyzed by *HindIII* restriction enzyme digestion and confirmed by DNA blotting with probes specific for the three chimeric ORFs **(Fig. 3B)**. Stability of the pBAC-BoHV-4 recombinant clones in *E. coli* cells (i.e., the absence of restriction pattern alterations upon artificial chromosome propagation) was verified by restriction enzyme digestion after multiple (up to 20) serial passages **(**see **Supplementary Fig. 5)**.

To produce viable, replication-competent recombinant viral particles, pBAC-BoHV-4-A-CMV-RHuT-gD-ΔTK, pBAC-BoHV-4-A-CMV-RRT-ΔTK, and pBAC-BoHV-4-A-CMV-RRT-Fc-ΔTK DNA constructs were electroporated into standard or *cre* recombinase-expressing BEK cells. The latter cells stably express the phage D1 *cre* recombinase [26] and allow for the site-specific removal of the floxed, GFP cassette-containing BAC sequence from the BAC-BoHV-4 genome. As a consequence of this removal and new cassette insertion, viral plaques generated on a BEK*cre* cell monolayer lost the

202 characteristic GFP fluorescence compared to parallel plaques seeded onto a standard BEK cell
203 monolayer **(Fig. 4A, D and G)**. Although viable BoHV-4-RHuT-gD, BoHV-4-RRT-gD and BoHV-4-
204 RRT-Fc virus particles were successfully reconstituted in BEK or BEK*cre* cells, as demonstrated by the
205 cytopathic effect (CPE) observed in the cell monolayer, it was of interest to determine their replication
206 properties with respect to the parental BoHV-4-A virus. As apparent in **Fig. 4B, E and H**, BoHV-4-
207 RHuT-gD, BoHV-4-RRT-gD and BoHV-4-RRT-Fc, all displayed a slower replication rate compared to
208 the reference BoHV-4-A type. Furthermore, as revealed by immunoblotting analysis of infected cell
209 extracts, they all expressed the corresponding HER-2 transgenes **(Fig. 4C, F and I)** and, as expected,
210 BoHV-4-RHuT-gD targeted transgene expression to the cell membrane **(**see **Supplementary Fig. 6).**
211
212 **Higher immunogenicity of HER-2 antigens delivered as BoHV-4 recombinant viral particles**
213 **compared to DNA immunization**
214 To test the immunogenicity of the different recombinant virus particles, four groups of BALB/c mice
215 (**7** animals/group) were vaccinated twice intraperitoneally (i.p.), at two weeks intervals, with BoHV-4-
216 RHuT-gD, BoHV-4-RRT-gD and BoHV-4-RRT-Fc, plus the unrelated BoHV-4-A29-gD control. Two
217 weeks after the second immunization, sera were collected and tested for the presence of anti-rat-Her-2
218 antibodies. No specific anti-rat-Her-2 humoral immune response was detected in mice vaccinated with
219 either BoHV-4-RRT-gD or BoHV-4-RRT-Fc. In contrast, BoHV-4-RHuT-gD viral particles elicited a
220 sustained anti-rat-Her-2 antibody response **(Fig. 5A)**, significantly higher (~2.5-fold) than the one
221 previously detected in BALB/c mice immunized with the pINT2-RHuT-gD plasmid ($p=0.02$) **(Fig.**
222 **2A)**. Also, while BoHV-4-A29-gD viral particles did not induce any appreciable cytotoxic response
223 against TYVPANASL-pulsed syngeneic splenocytes, all HER-2 containing recombinant BoHV-4 viral
224 particles induced a strong cytotoxicity **(Fig. 5B)**, significantly higher (~3-fold) than that induced by the
225 corresponding pINT2 plasmids delivered through DNA vaccination ($p=0.009$ for BoHV-4-RHuT-gD
226 *vs.* pINT2-RHuT-gD; $p=0.03$ for BoHV-4-RRT-gD *vs.* pINT2-RRT-gD; $p<0.0001$ for BoHV-4-RRT-
227 Fc *vs.* pINT2-RRT-Fc). Similarly, IFN-γ–producing cells were induced at high frequency by

228 TYVPANASL peptide restimulation of BoHV-4-HER-2- vaccinated mice **(Fig. 5C)**, with no
229 statistically significant difference between the three experimental groups.
230
231 **BoHV-4-RHuT-gD affords a significant protection against rat-HER-2-driven mammary**
232 **carcinogenesis in BALB-neuT mice.**
233 In HER-2-tolerant BALB-neuT mice, similarly to what we observed after vaccination with pINT2
234 plasmid DNA (**Supplementary Fig. 4**), only BoHV-4-RHuT-gD (*i.e.*, BoHV-4-A containing the
235 RHuT-gD expression cassette) effectively induced anti-rat-Her-2 antibodies, at levels considerably
236 higher (~**3** folds) than those elicited by pINT2 **(Fig. 6A)**. The superior immunogenicity of BoVH-4-
237 RHuT-gD is also supported by the earlier appearance of anti-rat Her-2 antibodies, which were already
238 well detectable after the first vaccination and increased thereafter, reaching titers significantly higher
239 than those elicited by pINT2-RHuT-gD ($p<0.0001$). Most importantly, the presence of anti-rat-Her-2
240 antibodies in sera from BALB-neuT mice vaccinated with BoHV-4-RHuT-gD correlated with a
241 significant delay of mammary tumor appearance. In fact, 50% of BoHV-4-RHuT-gD-vaccinated
242 BALB-neuT mice were completely tumor-free at week 30, when 100% of BoHV-4-RRT-gD- and
243 BoHV-4-RRT-Fc-vaccinated animals already displayed at least one palpable tumor **(Fig. 6B)**.
244

DISCUSSION

The aim of this study was to investigate the potential of BoHV-4 as a safe, potent and large-capacity vaccine vector able to deliver HER-2-derived engineered antigens and to protect HER-2 transgenic, BALB-neuT mice from autochthonous mammary cancer. BALB-neuT mice were used as a model system because they share a number of features with human breast cancer. In fact, following multi-step progression [15], each BALB-neuT mammary gland spontaneously develops an independent rat-Her-2^+tumor [12, 41], which becomes invasive and metastatizes to the bone marrow first and subsequently to the lungs [42]. Moreover, similarly to patients with rat Her-2^+ carcinomas, BALB-neuT mice lack high-affinity, Her-2 peptide-recognizing cytotoxic T lymphocytes [14], with an expansion of T regulatory [15] and myeloid immature suppressor cells [43] during carcinogenesis progression. For all these reasons, BALB-neuT mice represent an excellent model system to set up and test novel therapeutic and immune-prophylactic approaches to control breast cancer [37].

In this system, BoHV-4-delivered, membrane-bound rat-human Her-2 proved to be superior to the same antigen delivered through DNA vaccination with regard to tolerance breaking, humoral immune response induction and prevention of mammary tumor formation.

Initially, CMV-RHuT-gD, CMV-RRT-gD and CMV-RRT-Fc expression cassettes were successfully tested in terms of immune response by DNA vaccination. While all plasmids were able to induce a significant anti-rat Her-2 cellular immune response, only mice vaccinated with pINT-2-RHuT-gD induced a significant production of anti-rat Her-2 antibodies. As expected and already seen in other rat-HER-2 transgenic (CB6F1-neuT) mice vaccinated with a DNA plasmid coding for RHuT, the antibody titer measured in BALB-neuT mice was significantly lower than that of BALB/c mice, being the former deeply tolerant to rat-Her-2 protein [21]. We then constructed the three corresponding BoHV-4 vectors and evaluated their replication capacity by comparison with the parental BoHV-4-A strain. HER-2-containing recombinant viruses displayed a slower replication, likely attributable to a toxic effect caused by transgene overexpression. Despite their lower replication rate, however, all recombinant viruses abundantly expressed HER-2-derived transgenes in infected cells and triggered sustained T cell immune

responses in BALB/c mice. In contrast, and in keeping with the notion that sub-cellular localization of viral vectored transgenes critically affects antigen presentation to, and processing by, the immune system, membrane-targeted BoHV-4-RHuT-gD, but neither of the two secreted BoHV-4-HER-2 derivatives, was found to be capable of inducing a strong humoral anti-HER-2 response in BALB/c and BALB-neuT mice. In both mouse strains, the intensity of this response was significantly higher than that observed in mice vaccinated with the RHuT-encoding pINT-2 plasmid and an earlier anti-rat Her-2 antibody response, already detectable after the first vaccination, was observed in BALB-neuT mice. This sustained antibody production likely explains the striking delay in mammary cancer appearance brought about by BoHV-4-RHuT-gD vaccination. In fact, anti-rat Her-2 antibodies have previously been shown to cause a marked downregulation and cytoplasmic confinement of rat Her-2 both *in vitro* [13, 41] and *in vivo* [12, 21], with a concomitant impairment of Her-2 mediated PI3K/Akt signaling [44]. In addition, anti-Her-2 antibodies may activate complement-mediated lysis and antibody-dependent cytotoxicity [12, 21].

Various anti-Her-2 vaccine formulations have been tested in recent years, both in preclinical cancer models and in the clinic. These include allogenic Her-2$^+$ tumor cells [45-48], Her-2 peptide-presenting autologous dendritic cells [48, 49], Her-2 protein/peptide immunogens [50, 51], Her-2-based DNA vaccines [12, 21, 23, 41, 52], virus-like particles carrying Her-2 [53, 54] and even a chimeric recombinant Her-2 antigen expressed by an attenuated strain of *Listeria monicytogenes* [55]. Viral delivery vectors, instead, have received much less attention, recombinant vaccinia [56, 57] and adenovirus based vectors are the only viral vectors tested, with quite encouraging results, so far [58, 59]. This likely reflects potential concerns with safety and anti-vector immunity. Since risk associated with virus-mediated delivery represents a major issue in viral vector development, attenuation is usually regarded as a highly desirable feature and many efforts are directed toward the development of highly attenuated viral strains with decreased virulence. In this study, we took advantage of the natural non-pathogenicity of BoHV-4, which was previously proved in both standard and genetically modified mouse strains [28, 33]. Further to this point, we also previously inoculated high BoHV-4 doses intracerebrally with no apparent negative side-effect, and found that the

297 virus effectively transduced brain cells in the area of inoculation, leading to high-level expression of the
298 GFP transgene [60]. Therefore, BoHV-4 naturally behaves as a replication-incompetent viral vector that
299 does not require further attenuation. One other major advantages of BoHV-4 is its natural inability to
300 induce serum neutralizing antibody responses. This alleviates most concerns regarding the occurrence
301 of pre-existing, host anti-vector antibodies (as it is the case for adenovirus-based vectors) and allows for
302 multiple immunizations, if required.
303 In conclusion, our study highlights the favorable properties and potential advantages of BoHV-4 as a
304 highly effective viral vector for cellular Her-2 delivery in order to achieve mammary cancer prophylaxis
305 through a potential one-shot active immunization. Given the previous demonstration of the oncolytic
306 properties of BoHV-4 [29], future work will address the feasibility (and efficacy) of combined
307 prophylactic and therapeutic approaches based on the use of this particular viral vector.
308
309

Materials and Methods

Cell lines

Bovine embryo kidney [(BEK) from Dr. M. Ferrari, Istituto Zooprofilattico Sperimentale, Brescia, Italy; (BS CL-94)], BEK expressing cre recombinase (BEK cre) [26] , Human Embryo Kidney 293T [(HEK 293T) ATCC: CRL-11268] , Mus musculus mammary gland [(NMuMG) ATCC: CRL-1636] and NIH3T3 murine fibroblasts expressing rat-Her-2 protein (3T3/NKB cells) [61] cell lines were cultured in complete growth medium Eagle's minimal essential medium (EMEM, Lonza) containing 10% fetal bovine serum (FBS), 2 mM of L-glutamine (SIGMA), 100 IU/mL of penicillin (SIGMA), 100 µg/mL of streptomycin (SIGMA) and 2.5 µg/mL of Amphotericin B (SIGMA) and incubated at 37°C, 5% CO2.

PCR

The 2067 pb rat-human transmembrane protein (RHuT) and the 1250 pb rat extracellular domain (ECD) of rat Her-2 protein (RRT) were amplified from pVAX RHut plasmid [62] with NheI-RHut sense (5'- CCC*GCTAGC*CCACCATGATCATCATGGAGCTGGCGGCC-3') and SalI-RHut antisense (5'-CCCCGA*GTCGAC*CTTCCGGATCTTCTGCTGCCGTCG-3') and with NheI-RRT sense (5'-CCC*GCTAGC*CCACCATGATCATCATGGAGCTG-3') and SalI-RRT antisense (5'-CCCCGA*GTCGAC*TGTGATCTCCTCCAGGGTTTCGAACACTTGGAG3') primer pairs, respectively.

The PCR amplification reactions were carried out in a final volume of 50 µl, containing 10 mM Tris–hydrochloride pH 8.3, 0.2mM deoxynucleotide triphosphates, 3 mM MgCl2, 50 mM KCl and 0.25 µM of each primer. One hundred nanograms of DNA was amplified over 35 cycles, each cycle consisting of denaturation at 94°C for 1 min, primer annealing at 55°C for 1 min and chain elongation with 1U of Pfu DNA polymerase (Fermentas) at 72°C for 150 sec, in the case of RHut, and at 72°C for 90 sec, in the case of RRT. The so generated 2067 bp and 1250 pb amplicons were then checked in 1% agarose

gel and visualized after ethidium bromide staining in 1× TAE buffer (40 mM Tris-acetate, 1 mM EDTA).

Constructs generation

The NheI-RHut-SalI amplified fragment (2067 pb) was firstly sub-cloned inside the previously NheI/SalI digested pIgkE2gD106, an eukaryotic expression vector containing a gD_{106} epitope of Bovine herpesvirus 1 glycoprotein D, successfully used as a tag during the cloning [35]. The obtained pIgkRHuTgD_{106} was subsequently digested with NheI/BamHI to insert the 2169 fragment RHutgD_{106} into pEGFP-C1 vector (Addgene), digested with the same enzymes, to remove EGFP gene and to generate pCMVRHuTg$D_{106.}$ Finally, the 2421 pb Nhe/MluI-blunt ended fragment, containing RHuTgD_{106} with Simian Virus 40 poly A, was excised and inserted inside pINT2EGFPTK shuttle vector [24], cut with NheI/SmaI restriction enzymes, to obtain pINT2-RHuT-gD.

The amplified NheI-RRT-SalI (1250 pb) fragment was sub-cloned into NheI/SalI previously digested pIgkE2gD106 [35] and pIgkE2Fc, an eukaryotic expression vector expressing the crystallizable fragment (Fc) of mouse Immunoglobulin, used as a tag and soluble secreted frgment. RRT-gD106 (1352 pb) and RRTFc (1992 pb) were excised with the double digestion NheI/BamHI and inserted into NheI/BamHI digested pEGFP-C1 (Addgene), to remove EGFP gene and generate pCMV-RRT-gD106 and pCMV-RRT-Fc. NheI/MluI-blunt ended fragments containing RRT-gD106 (1604 pb) or RRT-Fc (2244), containing the Simian Virus 40 poly A, were excised and inserted inside pINT2EGFPTK shuttle vector [24], cut with NheI/SmaI restriction enzymes, to obtain pINT2-RRT-gD and pINT2-RRT-Fc.

Transient Transfection

Confluent HEK293T cells were seeded into 6 well plates ($3x10^5$ cells/well) and incubated at 37 °C with 5% CO_2; when the cells were sub-confluent the culture medium was removed and the cells were transfected with pINT2-RHuT-gD, pINT2-RRT-gD and pINT2-RRT-Fc, using Polyethylenimine (Pei)

362 transfection reagent (Polysciences, Inc.). Briefly, 3 μg of DNA were mixed with 7,5 μg PEI (1mg/mL)
363 (ratio 1:2.5 DNA- Pei) in 200 μL of Dulbecco's modified essential medium (DMEM) at high glucose
364 percentage (Euroclone) without serum. After 15 min at RT, 800 μL of medium without serum were
365 added and the transfection solution was transferred to the cells and left on the cells for 6 h at 37°C with
366 5% CO_2 in air, in a humidified incubator. The transfection mixture was then replaced with fresh
367 medium (EMEM, with 10% FBS, 50 IU/mL of penicillin, 100 μg/mL of streptomycin and 2.5 μg/mL
368 of Amphotericin B) and incubated for 24 h at 37°C with 5% CO_2.
369
370 **Viruses**
371 BoHV-4-RHuT-gD, BoHV-4-RRT-gD, BoHV-4-RRT-Fc and BoHV-4-A were propagated by
372 infecting confluent monolayers of BEK cells at a multiplicity of infection (MOI) of 0.5 50% tissue
373 culture infectious doses ($TCID_{50}$) per cell and maintained in medium with only 2% FBS for 2 h. The
374 medium was then removed and replaced with fresh EMEM containing 10% FBS. When the cytopathic
375 effect (CPE) interested the majority of the cell monolayer (~72 h post infection), the virus was prepared
376 by freezing and thawing cells three times and pelleting the virions through a 30% sucrose cushion, as
377 described previously [60]. Virus pellets were then resuspended in cold EMEM without FBS. $TCID_{50}$ were
378 determined with BEK cells by limiting dilution.
379
380 **Western Immunoblotting**
381 Protein cell extracts were obtained from a 6-well confluent plate of HEK293T transfected with pINT2-
382 RHuT-gD, pINT2-RRT-gD and pINT2-RRT-Fc and from 25-cm^2 confluent flasks of BEK infected
383 with BoHV-4-RHuT-gD, BoHV-4-RRT-gD, BoHV-4-RRT-Fc by adding 100 μL of cell extraction
384 buffer (50 mM Tris–HCl, 150 mM NaCl, and 1% NP-40; pH 8). A 10% SDS–PAGE gel
385 electrophoresis was used to analyze cell extracts containing 50 μg of total protein, after protein transfer
386 in nylon membranes by electroblotting, the membranes were incubated with primary bovine anti

BoHV-1 glycoprotein D monoclonal antibody (clone 1B8-F11; VRMD, Inc., Pullman, WA), diluited 1:15.000, and then with a secondary antibody probed with horseradish peroxidase-labelled anti-mouse immunoglobulin (A 9044; Sigma), diluited 1:10.000, to be visualized by enhanced chemiluminescence (ECL Kit; Pierce). pINT2-RRT-Fc and BoHV-4-RRT-Fc protein extracts were directly incubated with the secondary antibody probed with horseradish peroxidase-labelled anti-mouse immunoglobulin (A 9044; Sigma), recognizing the Fc tag.

BAC Recombineering and selection

Recombineering was performed as previously described [40] with some modifications. Five hundred microliters of a 32°C overnight culture of SW102 containing BAC-BoHV-4-A-Kana-GalKΔTK, were diluted in 25 ml Luria–Bertani (LB) medium with or without chloramphenicol (SIGMA) selection (12.5 mg/ml) in a 50 mL baffled conical flask and grown at 32°C in a shaking water bath to an OD_{600} of 0.6. Then, 10 mL were transferred to another baffled 50 mL conical flask and heat-shocked at 42°C for exactly 15 min in a shaking water bath. The remaining culture was left at 32°C as the un-induced control. After 15 min the two samples, induced and un-induced, were briefly cooled in ice/water bath slurry and then transferred to two 15 mL Falcon tubes and pelleted using 5000 r.p.m. (eppendorf centrifuge) at 0°C for 5 min. The supernatant was poured off and the pellet was resuspended in 1mL ice-cold ddH_2O by gently swirling the tubes in ice/water bath slurry. Subsequently, 9 mL ice-cold ddH_2O were added and the samples pelleted again. This step was repeated once more, the supernatant was removed and the pellet (50 µL each) was kept on ice until electroporated with gel-purified PvuI (Fermentas) linearized pINT2-RHuT-gD, pINT2-RRT-gD and pINT2-RRT-Fc. An aliquot of 25 µl was used for each electroporation in a 0.1 cm cuvette at 25 µF, 2.5 kV and 201Ω. After electroporation, for the counter selection step, the bacteria were recovered in 10 mL LB in a 50 mL baffled conical flask and incubated for 4.5 h in a 32°C shaking water bath. Bacteria serial dilutions were plated on M63 minimal medium plates containing 15g/L agar, 0.2% glycerol, 1mg/L D-biotin, 45mg/L L-leucine,

0.2% 2- deoxy-galactose and 12.5 mg/mL chloramphenicol. All the complements for M63 medium were purchased from SIGMA.

Plates were incubated 3–5 days at 32°C; then several selected colonies were picked up, streaked on McConkey agar indicator plates (DIFCO, BD Biosciences) containing 12.5 mg/mL of chloramphenicol and incubated at 32°C for 3 days until white colonies appeared. White colonies were grown in duplicate for 5–8 h in1mL of LB containing 50 mg/mL of kanamycin (SIGMA) or LB containing 12.5 mg/mL of chloramphenicol. Only those colonies that were kanamycin negative and chloramphenicol positive were kept and grown overnight in 5 mL of LB containing 12.5 mg/mL of chloramphenicol. BAC DNA was purified and analyzed through HindIII restriction enzyme digestion. DNA was separated by electrophoresis overnight in a 1% agarose gel, stained with ethidium bromide, and visualized to UV light.

Original detailed protocols for recombineering can also be found at the recombineering website (http://recombineering.ncifcrf.gov).

Non isotopic Southern blotting

DNA from 1% agarose gel was capillary transferred to a positively charged nylon membrane (Roche), and cross-linked by UV irradiation by standard procedures [26].

The membrane was pre-hybridized in 50 mL of hybridization solution (7% SDS, 0.5 M phosphate, pH 7.2) for 1 h at 65°C in a rotating hybridization oven (Techna instruments). The 1250 bp amplicon for RRT digoxigenin-labeled probe was generated by PCR with the primers NheI-RRT sense and SalI-RRT antisense, as previously described [27]. PCR amplification was carried out in a final volume of 50 µL of 10 mM Tris–HCl, pH 8.3, containing 0.2 mM deoxynucleotide triphosphates, 0.02 mM alkaline labile digoxigenin-dUTP (Roche), 3 mM $MgCl_2$, 50 mM KCl, and 0.25 µM of each primer over 35 cycles, each cycle consisting of denaturation at 94°C for 1 min, primer annealing at 55°C for 1 min, and chain elongation with 1 U of Taq polymerase (Thermoscientific) at 72°C for 90 sec. A parallel reaction omitting digoxigenin dUTP was performed, because digoxigenin incorporation into the amplicon can

438 be checked through the size shift of the amplicon by gel electrophoresis. Five microliters of the probe
439 were added to 500 μL of dH_2O into a screw-cap tube, denatured in boiling water for 5 min, and cooled
440 down on ice for another 2 min. Denatured probe was added to 50 mL of pre-heated 65°C hybridization
441 solution (7% SDS, 0.5 M phosphate, pH 7.2 and 1 mM EDTA) to the pre-hybridized membrane and
442 hybridized overnight at 65°C in a rotating hybridization oven (Techna Instruments). Following
443 hybridization, the membrane was washed twice for 30 min with 100 mL of washing solution I (0.5×
444 SSC [1× SSC is 0.15 M NaCl plus 0.015 M sodium citrate] and 0.1% SDS) and twice for 30 min with
445 100 mL of washing solution II (40 mM phosphate, pH 7.2, 0.05% SDS) at 65 °C. On a freshly washed
446 dish, the membrane was incubated for 30 min at room temperature in 100 mL of blocking solution
447 (100 mM maleic acid, pH 7.5, 150 mM NaCl, 1% blocking reagent [Roche]). Anti-digoxigenin Fab
448 fragment (150 U/200 μL [Roche]), diluted 1:15.000 in 50 mL of blocking solution, was applied to the
449 membrane for 30 min under gentle shaking at room temperature and washed twice for 15 min with 100
450 mL of washing solution (100 mM maleic acid, pH 7.5, 150 mM NaCl, 0.3% Tween 20). Detection was
451 performed following equilibration of the membrane in detection buffer (100 mM Tris–HCl, pH 9.5, 1
452 mM EDTA) for 2 min at room temperature. Chemiluminescent substrate (CSPD, Roche) was added by
453 scattering the drops over the surface of the membrane after placement of the membrane between two
454 plastic sheets, and any bubbles present under the sheet were eliminated with a damp lab tissue to create
455 a liquid seal around the membrane. Signal detection was obtained, exposing the membrane to X-ray
456 film. The exposure time was adjusted with the intensity of the signal.
457
458 **Cell culture electroporation and recombinant virus reconstitution**
459 BEK or BEK*cre* cells were maintained as a monolayer with complete EMEM growth medium with 10%
460 FBS, 2 mM L-glutamine, 100 IU/mL penicillin and 100 μg/mL streptomycin.
461 When cells were sub-confluent (70–90%) they were split to a fresh culture vessel (i.e., every 3–5 days)
462 and were incubated at 37°C in a humidified atmosphere of 95% air–5% CO2.

463 BAC DNA (5 μg) was electroporated in 600 μL DMEM without serum (Equibio apparatus, 270 V, 960
464 mF, 4-mm gap cuvettes) into BEK and/or BEK*cre* cells from a confluent 25-cm^2 flask. Electroporated
465 cells were returned to the flask, after 24 h the medium was replaced with fresh medium, and cells were
466 split 1:2 when they reached confluence at 2 days post-electroporation. Cells were left to grow until the
467 appearance of CPE. Recombinant viruses were propagated by infecting confluent monolayers of BEK
468 cells at a M.O.I. of 0.5 $TCID_{50}$ per cell and maintaining them in MEM with 10% FBS for 2 h.
469
470 **Viral growth curves**
471 BEK cells were infected with BoHV-4-A, BoHV-4-RHuT-gD, BoHV-4-RRT-gD, BoHV-4-RRT-Fc at
472 a M.O.I. of 0,1 TCID50/cell and incubated at 37°C for 4 h. Infected cells were washed with serum-free
473 EMEM and then overlaid with EMEM containing 10% FBS, 2 mM Lglutamine, 100 IU/mL penicillin,
474 100 μg/mL streptomycin and 2.5 μg/mL Amphotericin B. The supernatants of infected cultures were
475 harvested after 24, 48, 72 and 96 h, and the amount of infectious virus was determined by limiting
476 dilution on BEK cells.
477
478 **Mice**
479 BALB/c (Charles River) and BALB-neuT (Ariano Irpino, Italy) [63] mice were bred under specific
480 pathogen-free conditions (Allentown Caging Equipment, Allentown, NJ, USA) at the Molecular
481 Biotechnology Center (Torino, Italy) and treated according to the European Guidelines and policies, as
482 approved by the University of Torino Ethical Committee. To assess mammary tumor incidence BALB-
483 neuT females were inspected weekly by palpation, and progressively growing masses with a mean
484 diameter of >1 mm were regarded as tumors. Each tumor mass was measured with a calliper in the two
485 perpendicular diameters. Growth was monitored until all 10 mammary glands displayed a tumor or
486 until a tumor exceeded a mean diameter of 10 mm, at which time mice were sacrificed for humane
487 reasons.
488

Mice immunization

Recombinant pINT2 plasmids were purified by large scale preparation using the EndoFree Plasmid Giga kits (Qiagen, Inc., CA, USA). 10 week-old BALB/c and BALB-neuT mice were anesthetized by intramuscular injection (i.m.) of 40 μL of a solution containing 5,7 μL of Zoletil 100 (Vibrac, Milano, Italia), 3,5 μL of Rompum (Bayer, Milano, Italia) and 37,5 μL of Phosphate Buffer Saline (PBS) (GIBCO, Grand Island, NY, USA). Anesthetized mice were injected in the quadriceps muscle with 50 μg of plasmid DNA diluted in 20 μL of saline solution. Immediately after injection, two 25-ms trans-cutaneous electric low voltage pulses with amplitude of 150 V and a 300 ms interval were administered at the injection site via a multiple needle electrode connected to the Cliniporator™ (IGEA s.r.l., Carpi, Italy). The DNA vaccination course consisted of two i.m. injections of plasmid followed by electroporation repeated with an interval of 14 days.

10^6 $TCID_{50}$ recombinant BoHV-4 viral particles were diluted in 200 μL of Dubecco's Modified Eagle Medium (DMEM; Gibco, Rockville, MD) and injected intraperitoneal (i.p.) twice at two weeks interval in groups of 10 week-old BALB/c or BALB-neuT females.

Anti-rat-Her-2 antibody response

Two weeks after the second immunization, mice were bled and their sera were tested by flow cytometry for their ability to bind 3T3/NKB cells [61]. Briefly, sera diluted 1:100 in PBS were incubated for 30 min at 4°C with 2 x 10^5 3T3/NKB cells pre-treated with Fc receptor blocker (CD16/CD32; Pharmingen, St. Diego, CA) for 5 min at 4°C. The Ab4 mAb (Calbiochem, San Diego, CA), was used as positive control for rat Her-2 positivity. After washes with PBS containing 2% bovine serum albumin (BSA, Sigma-Aldrich, Milano, Italy) and 0.1% NaN3 (Sigma-Aldrich) (wash solution) cells were incubated with 1:50 dilution of a FITC-conjugate anti-mouse immunoglobulin G (IgG) Fc antibody (DakoCytomation, Milano, Italy) for 30 min at 4°C. Washed cells were then acquired and analyzed on the CyAn ADP using Summit 4.3 software (DakoCytomation, Heverlee, Belgium). The results were expressed as Mean Fluorescence Intensity (MFI).

Anti-rat-Her-2 cellular immune response

To prepare target cells for *in vivo* cytotoxicity detection, spleens from BALB/c and BALB-neuT mice were mechanically dissociated and the erythrocytes were removed from the cells suspension by osmotic lysis. Cells were then washed and labeled with two different CFSE (carboxyfluorescein-diacetate-succinimidyl ester) (Molecular Probes Invitrogen, Carlsbad, CA) concentration (5 and 0.5 μM). Cells labelled with 5 μM CFSE ($CFSE_{high}$ cells) were also pulsed with the rat-Her-$2H2^d$ dominant TYVPANASL peptide (INBIOS Srl) at a concentration of 15 μg/mL for 1 h at 37°C; those labelled with 0.5 μM CFSE ($CFSE_{low}$ cells) were left unpulsed. 10 x 10^6 $CFSE_{high}$ cells plus 10 x 10^6 $CFSE_{low}$ cells were injected in the tail vein of vaccinated mice. Forty eight h after spleen cells injection, mice were sacrificed and the presence of $CFSE_{high}$ and $CFSE_{low}$ in the spleen was measured by using a CyAn ADP Flow Cytometer (DakoCytomation). The percentage of the low peaks was normalized on control untreated low peaks and consequently the specific cytolytic activity was calculated as percentage of lysis as following described: 100 - {[($CFSE_{low}$ untreated cells/ $CFSE_{low}$ experimental cells) x $CFSE_{high}$ experimental cells] x 100} / $CFSE_{high}$ untreated cells.

To measure the number of rat-Her-2specific IFN-γ releasing T lymphocytes a mouse IFN-γ ELISPOT assay kit purchased from BD Biosciences (San Jose, CA, USA) was used. Briefly, two weeks after the vaccination course, 0.5 x 10^6 spleen cells were added to the wells of 96-well HTS IP plates (Millipore, Billerica, MA) pre-coated with 5 μg/mL of rat anti-mouse IFN-γ (clone R4-6A2, BD Biosciences, San Jose, CA, USA). Spleen cells were stimulated with 15 μg/mL of TYVPANASL peptide (INBIOS Srl, Napoli, Italy) for 24 h at 37°C in a humidified 5% CO2 atmosphere. Concanavalin A (Sigma-Aldrich) at the concentration of 2 μg/mL and RPMI-1640 medium (Sigma-Aldrich) alone were used as positive and negative control, respectively. IFN-γ spots were scanned and counted using an ImmunoSpot Image Analyzer software (Aelvis, Germany). Results were plotted as median of spot values among triplicates.

Immunofluorescence assay

For rat Her-2 detection, 4×10^5 Nmug cells were plated on glass coverslips and left to adhere overnight at 37 °C in a 5% CO_2 incubator. The next day, cells were infected for 24 hours) with 0,5 TCID50/cell of BoHV-4-RHuT-gD or with the same TCID50/cell of BoHV-4-RHuT-gD inactivated at 70°C for 30 minutes. After infection, cells were fixed with 4% formalin (Sigma-Aldrich) solution in PBS for 5 minutes at room temperature, washed twice with PBS and blocked with 10% bovine serum albumin (BSA, Sigma-Aldrich) in PBS for 40 minutes at room temperature. Her-2 was detected incubating coverslips with an anti rat/Her-2 monoclonal antibody (1:20, clone number, Calbiochem, San Diego, CA) for 1 hour at room temperature in PBS containing 1% BSA. Cells were rinsed twice with PBS and then incubated with AlexaFluor488 goat anti-mouse (1:1000, clone A11017, Invitrogen) in PBS containing 1% BSA. Cells were rinsed three times with PBS and nuclei were counterstained with DAPI (Invitrogen). Coverslips were air dried and mounted with Fluoromount mounting medium (Sigma-Aldrich) and visualized with Apotome fluorescence microscope (Leica,). Photographs were taken using a digital CCD camera and images were processed using the AxioVision software (Zeiss, V. 4.4).

FACS analysis

For rat Her-2 detection, 4×10^5 Nmug cells were plated and left to adhere overnight at 37 °C in a 5% CO_2 incubator. The next day, cells were infected for 24 hours with 0,5 TCID50/cell of BoHV-4-RHuT-gD or with the same TCID50/cell of BoHV-4-RHuT-gD inactivated at 70°C for 30 minutes. After infection, cells were detached with tripsin 1X (Invitrogen o Sigma), incubated with Fc receptor blocker (CD16/CD32; Pharmingen, St. Diego, CA) for 5 min at 4°C to block aspecific site. Her-2 was detected incubating cells with an anti rat/Her-2 monoclonal antibody (1:25, clone number, Calbiochem, San Diego, CA) for 30 min at 4°C. Then cells were washed with PBS containing 2% bovine serum albumin (BSA, Sigma-Aldrich, Milano, Italy) and 0.1% NaN3 (Sigma-Aldrich) (wash solution) and incubated with 1:50 dilution of a FITC-conjugate anti-mouse immunoglobulin G (IgG) Fc antibody (DakoCytomation, Milano, Italy) for 30 min at 4°C. Washed cells were then acquired and analyzed on the CyAn ADP using Summit 4.3 software (DakoCytomation, Heverlee, Belgium).

Statistical analysis

Statistical differences were evaluated using GraphPad software 5.0 (GraphPad Inc.). The Mantel-Cox log-rank test was used to evaluate the differences in the tumor incidence between different experimental groups. The two-tailed unpaired Student's t test was used to evaluate differences in the antibody titer, % of lysis and number of IFN-γ secreting T cells between different experimental groups.

Acknowledgments

This work was supported by grants from the Italian Association for Cancer Research (AIRC, grant IG 12956 and IG 11675), the Compagnia di San Paolo (Progetti di Ricerca Ateneo/CSP, TO_call02_2012_0026), the University of Torino (Italy), the Italian Ministry for Education, University and Research (MIUR), Grant # 2010LLXR94_004 and University of Parma (Italy).

581 **References**

582 1. Whenham N, D'Hondt V, Piccart MJ. HER2-positive breast cancer: from trastuzumab to
583 innovatory anti-HER2 strategies. Clinical breast cancer 2008; 8:38-49.

584 2. Slamon DJ, Clark GM. Amplification of c-erbB-2 and aggressive human breast tumors? Science
585 1988; 240:1795-8.

586 3. Slamon DJ, Godolphin W, Jones LA, Holt JA, Wong SG, Keith DE, et al. Studies of the HER-
587 2/neu proto-oncogene in human breast and ovarian cancer. Science 1989; 244:707-12.

588 4. Gusterson BA, Gelber RD, Goldhirsch A, Price KN, Save-Soderborgh J, Anbazhagan R, et al.
589 Prognostic importance of c-erbB-2 expression in breast cancer. International (Ludwig) Breast Cancer
590 Study Group. Journal of clinical oncology : official journal of the American Society of Clinical
591 Oncology 1992; 10:1049-56.

592 5. Yarden Y, Sliwkowski MX. Untangling the ErbB signalling network. Nature reviews Molecular
593 cell biology 2001; 2:127-37.

594 6. Atalay G, Cardoso F, Awada A, Piccart MJ. Novel therapeutic strategies targeting the epidermal
595 growth factor receptor (EGFR) family and its downstream effectors in breast cancer. Annals of
596 oncology : official journal of the European Society for Medical Oncology / ESMO 2003; 14:1346-63.

597 7. Harari D, Yarden Y. Molecular mechanisms underlying ErbB2/HER2 action in breast cancer.
598 Oncogene 2000; 19:6102-14.

599 8. Hudis CA. Trastuzumab--mechanism of action and use in clinical practice. The New England
600 journal of medicine 2007; 357:39-51.

601 9. McArthur HL, Hudis CA. Breast cancer chemotherapy. Cancer J 2007; 13:141-7.

602 10. El-Sahwi K, Bellone S, Cocco E, Cargnelutti M, Casagrande F, Bellone M, et al. In vitro activity
603 of pertuzumab in combination with trastuzumab in uterine serous papillary adenocarcinoma. British
604 journal of cancer 2010; 102:134-43.

605 11. Higa GM, Abraham J. Lapatinib in the treatment of breast cancer. Expert review of anticancer
606 therapy 2007; 7:1183-92.

12. Quaglino E, Iezzi M, Mastini C, Amici A, Pericle F, Di Carlo E, et al. Electroporated DNA vaccine clears away multifocal mammary carcinomas in her-2/neu transgenic mice. Cancer research 2004; 64:2858-64.

13. Quaglino E, Rolla S, Iezzi M, Spadaro M, Musiani P, De Giovanni C, et al. Concordant morphologic and gene expression data show that a vaccine halts HER-2/neu preneoplastic lesions. The Journal of clinical investigation 2004; 113:709-17.

14. Rolla S, Nicolo C, Malinarich S, Orsini M, Forni G, Cavallo F, et al. Distinct and non-overlapping T cell receptor repertoires expanded by DNA vaccination in wild-type and HER-2 transgenic BALB/c mice. J Immunol 2006; 177:7626-33.

15. Ambrosino E, Spadaro M, Iezzi M, Curcio C, Forni G, Musiani P, et al. Immunosurveillance of Erbb2 carcinogenesis in transgenic mice is concealed by a dominant regulatory T-cell self-tolerance. Cancer research 2006; 66:7734-40.

16. Holmgren L, Ambrosino E, Birot O, Tullus C, Veitonmaki N, Levchenko T, et al. A DNA vaccine targeting angiomotin inhibits angiogenesis and suppresses tumor growth. Proceedings of the National Academy of Sciences of the United States of America 2006; 103:9208-13.

17. Pannellini T, Spadaro M, Di Carlo E, Ambrosino E, Iezzi M, Amici A, et al. Timely DNA vaccine combined with systemic IL-12 prevents parotid carcinomas before a dominant-negative p53 makes their growth independent of HER-2/neu expression. J Immunol 2006; 176:7695-703.

18. Rizzuto GA, Merghoub T, Hirschhorn-Cymerman D, Liu C, Lesokhin AM, Sahawneh D, et al. Self-antigen-specific CD8+ T cell precursor frequency determines the quality of the antitumor immune response. The Journal of experimental medicine 2009; 206:849-66.

19. Engelhorn ME, Guevara-Patino JA, Noffz G, Hooper AT, Lou O, Gold JS, et al. Autoimmunity and tumor immunity induced by immune responses to mutations in self. Nature medicine 2006; 12:198-206.

20. Luo W, Hsu JC, Kieber-Emmons T, Wang X, Ferrone S. Human tumor associated antigen mimicry by xenoantigens, anti-idiotypic antibodies and peptide mimics: implications for

633 immunotherapy of malignant diseases. Cancer chemotherapy and biological response modifiers 2005;
634 22:769-87.
635 21. Quaglino E, Mastini C, Amici A, Marchini C, Iezzi M, Lanzardo S, et al. A better immune
636 reaction to Erbb-2 tumors is elicited in mice by DNA vaccines encoding rat/human chimeric proteins.
637 Cancer research 2010; 70:2604-12.
638 22. Bolli E, Quaglino E, Arigoni M, Lollini PL, Calogero R, Forni G, et al. Oncoantigens for an
639 immune prevention of cancer. American journal of cancer research 2011; 1:255-64.
640 23. Jacob JB, Quaglino E, Radkevich-Brown O, Jones RF, Piechocki MP, Reyes JD, et al.
641 Combining human and rat sequences in her-2 DNA vaccines blunts immune tolerance and drives
642 antitumor immunity. Cancer research 2010; 70:119-28.
643 24. Donofrio G, Cavirani S, Simone T, van Santen VL. Potential of bovine herpesvirus 4 as a gene
644 delivery vector. Journal of virological methods 2002; 101:49-61.
645 25. Donofrio G, Sartori C, Ravanetti L, Cavirani S, Gillet L, Vanderplasschen A, et al.
646 Establishment of a bovine herpesvirus 4 based vector expressing a secreted form of the bovine viral
647 diarrhoea virus structural glycoprotein E2 for immunization purposes. BMC biotechnology 2007; 7:68.
648 26. Donofrio G, Sartori C, Franceschi V, Capocefalo A, Cavirani S, Taddei S, et al. Double
649 immunization strategy with a BoHV-4-vectorialized secreted chimeric peptide BVDV-E2/BoHV-1-gD.
650 Vaccine 2008; 26:6031-42.
651 27. Donofrio G, Franceschi V, Capocefalo A, Taddei S, Sartori C, Bonomini S, et al. Cellular
652 targeting of engineered heterologous antigens is a determinant factor for bovine herpesvirus 4-based
653 vaccine vector development. Clinical and vaccine immunology : CVI 2009; 16:1675-86.
654 28. Franceschi V, Capocefalo A, Calvo-Pinilla E, Redaelli M, Mucignat-Caretta C, Mertens P, et al.
655 Immunization of knock-out alpha/beta interferon receptor mice against lethal bluetongue infection
656 with a BoHV-4-based vector expressing BTV-8 VP2 antigen. Vaccine 2011; 29:3074-82.
657 29. Redaelli M, Franceschi V, Capocefalo A, D'Avella D, Denaro L, Cavirani S, et al. Herpes
658 simplex virus type 1 thymidine kinase-armed bovine herpesvirus type 4-based vector displays enhanced

659 oncolytic properties in immunocompetent orthotopic syngenic mouse and rat glioma models. Neuro-
660 oncology 2012; 14:288-301.
661 30. Donofrio G, Franceschi V, Lovero A, Capocefalo A, Camero M, Losurdo M, et al. Clinical
662 protection of goats against CpHV-1 induced genital disease with a BoHV-4-based vector expressing
663 CpHV-1 gD. PloS one 2013; 8:e52758.
664 31. Donofrio G, Martignani E, Poli E, Lange C, Martini FM, Cavirani S, et al. Bovine herpesvirus 4
665 based vector interaction with liver cells in vitro and in vivo. Journal of virological methods 2006;
666 136:126-36.
667 32. Donofrio G, Taddei S, Franceschi V, Capocefalo A, Cavirani S, Martinelli N, et al. Swine
668 adipose stromal cells loaded with recombinant bovine herpesvirus 4 virions expressing a foreign antigen
669 induce potent humoral immune responses in pigs. Vaccine 2011; 29:867-72.
670 33. Franceschi V, Stellari FF, Mangia C, Jacca S, Lavrentiadou S, Cavirani S, et al. In vivo image
671 analysis of BoHV-4-based vector in mice. PloS one 2014; 9:e95779.
672 34. Osorio FA, Reed DE. Experimental inoculation of cattle with bovine herpesvirus-4: evidence
673 for a lymphoid-associated persistent infection. American journal of veterinary research 1983; 44:975-80.
674 35. Capocefalo A, Franceschi V, Mertens PP, Castillo-Olivares J, Cavirani S, Di Lonardo E, et al.
675 Expression and secretion of Bluetongue virus serotype 8 (BTV-8)VP2 outer capsid protein by
676 mammalian cells. Journal of virological methods 2010; 169:420-4.
677 36. Franceschi V, Parker S, Jacca S, Crump RW, Doronin K, Hembrador E, et al. BoHV-4-Based
678 Vector Single Heterologous Antigen Delivery Protects STAT1(-/-) Mice from Monkeypoxvirus Lethal
679 Challenge. PLoS neglected tropical diseases 2015; 9:e0003850.
680 37. Quaglino E, Mastini C, Forni G, Cavallo F. ErbB2 transgenic mice: a tool for investigation of
681 the immune prevention and treatment of mammary carcinomas. Current protocols in immunology /
682 edited by John E Coligan [et al] 2008; Chapter 20:Unit 20 9 1- 9-10.
683 38. Franceschi V, Capocefalo A, Cavirani S, Donofrio G. Bovine herpesvirus 4 glycoprotein B is
684 indispensable for lytic replication and irreplaceable by VSVg. BMC veterinary research 2013; 9:6.

685 39. Capocefalo A, Mangia C, Franceschi V, Jacca S, van Santen VL, Donofrio G. Efficient
686 heterologous antigen gene delivery and expression by a replication-attenuated BoHV-4-based vaccine
687 vector. Vaccine 2013; 31:3906-14.
688 40. Warming S, Costantino N, Court DL, Jenkins NA, Copeland NG. Simple and highly efficient
689 BAC recombineering using galK selection. Nucleic acids research 2005; 33:e36.
690 41. Rovero S, Amici A, Di Carlo E, Bei R, Nanni P, Quaglino E, et al. DNA vaccination against rat
691 her-2/Neu p185 more effectively inhibits carcinogenesis than transplantable carcinomas in transgenic
692 BALB/c mice. J Immunol 2000; 165:5133-42.
693 42. Husemann Y, Geigl JB, Schubert F, Musiani P, Meyer M, Burghart E, et al. Systemic spread is
694 an early step in breast cancer. Cancer cell 2008; 13:58-68.
695 43. Melani C, Chiodoni C, Forni G, Colombo MP. Myeloid cell expansion elicited by the
696 progression of spontaneous mammary carcinomas in c-erbB-2 transgenic BALB/c mice suppresses
697 immune reactivity. Blood 2003; 102:2138-45.
698 44. Porzia A, Lanzardo S, Citti A, Cavallo F, Forni G, Santoni A, et al. Attenuation of PI3K/Akt-
699 mediated tumorigenic signals through PTEN activation by DNA vaccine-induced anti-ErbB2
700 antibodies. J Immunol 2010; 184:4170-7.
701 45. Dols A, Meijer SL, Smith JW, 2nd, Fox BA, Urba WJ. Allogeneic breast cancer cell vaccines.
702 Clinical breast cancer 2003; 3 Suppl 4:S173-80.
703 46. Dols A, Smith JW, 2nd, Meijer SL, Fox BA, Hu HM, Walker E, et al. Vaccination of women
704 with metastatic breast cancer, using a costimulatory gene (CD80)-modified, HLA-A2-matched,
705 allogeneic, breast cancer cell line: clinical and immunological results. Human gene therapy 2003;
706 14:1117-23.
707 47. Dols A, Meijer SL, Hu HM, Goodell V, Disis ML, Von Mensdorff-Pouilly S, et al.
708 Identification of tumor-specific antibodies in patients with breast cancer vaccinated with gene-modified
709 allogeneic tumor cells. J Immunother 2003; 26:163-70.

48. Park JW, Melisko ME, Esserman LJ, Jones LA, Wollan JB, Sims R. Treatment with autologous antigen-presenting cells activated with the HER-2 based antigen Lapuleucel-T: results of a phase I study in immunologic and clinical activity in HER-2 overexpressing breast cancer. J Clin Oncol 2007; 25:3680-7.

49. Occhipinti S, Sponton L, Rolla S, Caorsi C, Novarino A, Donadio M, et al. Chimeric rat/human HER2 efficiently circumvents HER2 tolerance in cancer patients. Clin Cancer Res 2014; 20:2910-21.

50. Kitano S, Kageyama S, Nagata Y, Miyahara Y, Hiasa A, Naota H, et al. HER2-specific T-cell immune responses in patients vaccinated with truncated HER2 protein complexed with nanogels of cholesteryl pullulan. Clinical cancer research : an official journal of the American Association for Cancer Research 2006; 12:7397-405.

51. Mittendorf EA, Holmes JP, Ponniah S, Peoples GE. The E75 HER2/neu peptide vaccine. Cancer Immunol Immunother 2008; 57:1511-21.

52. Aurisicchio L, Peruzzi D, Conforti A, Dharmapuri S, Biondo A, Giampaoli S, et al. Treatment of mammary carcinomas in HER-2 transgenic mice through combination of genetic vaccine and an agonist of Toll-like receptor 9. Clinical cancer research : an official journal of the American Association for Cancer Research 2009; 15:1575-84.

53. Andreasson K, Tegerstedt K, Eriksson M, Curcio C, Cavallo F, Forni G, et al. Murine pneumotropic virus chimeric Her2/neu virus-like particles as prophylactic and therapeutic vaccines against Her2/neu expressing tumors. International journal of cancer Journal international du cancer 2009; 124:150-6.

54. Tegerstedt K, Lindencrona JA, Curcio C, Andreasson K, Tullus C, Forni G, et al. A single vaccination with polyomavirus VP1/VP2Her2 virus-like particles prevents outgrowth of HER-2/neu-expressing tumors. Cancer research 2005; 65:5953-7.

55. Seavey MM, Pan ZK, Maciag PC, Wallecha A, Rivera S, Paterson Y, et al. A novel human Her-2/neu chimeric molecule expressed by Listeria monocytogenes can elicit potent HLA-A2 restricted CD8-positive T cell responses and impact the growth and spread of Her-2/neu-positive breast tumors.

Clinical cancer research : an official journal of the American Association for Cancer Research 2009; 15:924-32.

56. Masuelli L, Marzocchella L, Focaccetti C, Lista F, Nardi A, Scardino A, et al. Local delivery of recombinant vaccinia virus encoding for neu counteracts growth of mammary tumors more efficiently than systemic delivery in neu transgenic mice. Cancer immunology, immunotherapy : CII 2010; 59:1247-58.

57. Masuelli L, Fantini M, Benvenuto M, Sacchetti P, Giganti MG, Tresoldi I, et al. Intratumoral delivery of recombinant vaccinia virus encoding for ErbB2/Neu inhibits the growth of salivary gland carcinoma cells. Journal of translational medicine 2014; 12:122.

58. Gallo P, Dharmapuri S, Nuzzo M, Maldini D, Cipriani B, Forni G, et al. Adenovirus vaccination against neu oncogene exerts long-term protection from tumorigenesis in BALB/neuT transgenic mice. International journal of cancer Journal international du cancer 2007; 120:574-84.

59. Park JM, Terabe M, Steel JC, Forni G, Sakai Y, Morris JC, et al. Therapy of advanced established murine breast cancer with a recombinant adenoviral ErbB-2/neu vaccine. Cancer research 2008; 68:1979-87.

60. Donofrio G, Cavaggioni A, Bondi M, Cavirani S, Flammini CF, Mucignat-Caretta C. Outcome of bovine herpesvirus 4 infection following direct viral injection in the lateral ventricle of the mouse brain. Microbes and infection / Institut Pasteur 2006; 8:898-904.

61. Jacob J, Radkevich O, Forni G, Zielinski J, Shim D, Jones RF, et al. Activity of DNA vaccines encoding self or heterologous Her-2/neu in Her-2 or neu transgenic mice. Cell Immunol 2006; 240:96-106.

62. Marchini C, Kalogris C, Garulli C, Pietrella L, Gabrielli F, Curcio C, et al. Tailoring DNA Vaccines: Designing Strategies Against HER2-Positive Cancers. Frontiers in oncology 2013; 3:122.

63. Boggio K, Nicoletti G, Di Carlo E, Cavallo F, Landuzzi L, Melani C, et al. Interleukin 12-mediated prevention of spontaneous mammary adenocarcinomas in two lines of Her-2/neu transgenic mice. The Journal of experimental medicine 1998; 188:589-96.

FIGURE LEGENDS

Figure 1. Design and expression of Her-2 chimeric proteins. Diagrams (not to scale) of (**A**) pTK-CMV-RHuT-gD-TK (pINT2-RHuT-gD), (**B**) pTK-CMV-RRT-gD-TK (pINT2-RRT-gD) and (**C**) pTK-CMV-RRT-Fc-TK (pINT2-RRT-Fc) targeting vectors with expression cassettes under the control of the CMV promoter (pCMV, *blue*) and the bovine growth hormone polyadenylation signal (PA, *orange*). RHuT-gD (**A**) and RRT-gD (**B**) ORFs are tagged with the gD106 peptide (*red*), while the RRT-Fc ORF (**C**) was fused to a mouse IgG Fc encoding fragment (*grey*). All expression cassettes are flanked by BoHV-4 TK homologous sequences (*white*). The results of immunoblotting analyses conducted with an anti-gD106 antibody on HEK 293Tcells transfected with pINT2-RHuT-gD, pINT2-RRT-gD and pINT2-RRT-Fc are shown in panels **D-F**, respectively. Individual lanes were loaded with different amounts of total protein cell extract (5, 10 and 20 μg); cells transfected with pEGFP-1 served as negative controls (*Mock*).

Figure 2. Anti-rat-Her-2 immune responses induced by DNA vaccination with the different pINT2 expression plasmids. (**A**) Sera from BALB/c mice collected two weeks after the first (*grey dots*; n=6) and the second (*black dots*; n=6) vaccination were analyzed (at a dilution of 1:100) for the presence of specific anti-rat-Her-2 antibodies by flow cytometry. Results are expressed as mean fluorescence intensity (MFI) values for each serum. Horizontal lines represent median values (**: p=0.003, Student's t test). (**B**) *In vivo* cytotoxic responses against the $H2^d$ dominant, rat Her-2 TYVPANASL peptide measured two weeks after the second vaccination in mice (n=3) immunized with the indicated pINT2 plasmids; data are mean values ± SEM. (*: p=0.02; **: p=0.005; ***: p<0.0001; Student's t-test). (**C**) T-cell responses against the $H2^d$ dominant, rat Her-2 TYVPANASL peptide measured *in vitro*, two weeks after the second vaccination, in mice (n=3) immunized with the indicated pINT2 plasmids, using an IFN-γ-based ELISPOT assay. Data, expressed as SFU/$1x10^6$ SPC, are presented as mean ± SEM values (**: p=0.001, ***: p=0.0008; Student's t-test).

Figure 3. Recombinant BoHV-4 constructs. (**A**) Diagram (not to scale) illustrating the re-targeting event (i.e., replacement of the Kana/GalK cassette with the CMV-RHuT-gD, CMV-RRT-gD and CMV-RRT-Fc expression cassettes) generated by heat-inducible homologous recombination in SW102 *E. coli* cells containing pBAC-BoHV-4-A-TK-KanaGalK-TK. (B) Two representative, 2-deoxy-galactose resistant colonies for each recombinant pBAC-BoHV-4 genome, tested by *Hind*III restriction enzyme analysis and DNA blotting performed with a probe targeting the rat HER-2 portion of each chimeric ORF. The 2,650 bp band (circled in *yellow*) corresponding to the non-retargeted pBAC-BoHV-4-A-TK-KanaGalK-TK control is replaced by 2,825 bp, 3,642 bp and 3,464 bp bands (circled in *red*) in pBAC-BoHV-4-RRT-gD, pBAC-BoHV-4-RHuT-gD and pBAC-BoHV-4-RRT-Fc, respectively.

Figure 4. Reconstitution and characterization of recombinant viruses. Representative phase contrast and fluorescent microscopy images of the plaques formed by viable, reconstituted recombinant BoHV-4-RHuT-gD (**A**), BoHV-4-RRT-**Fc** (**D**) and BoHV-4-RRT-gD **(G)** after electroporation of the corresponding BAC DNA clones into BEK or *BEKcre* cells (magnification, ×10). Replication rates of BoHV-4-RHuT-gD, BoHV-4-RRT-Fc and BoHV-4-RRT-gD grown in BEK cells are shown in panels **B**, **E** and **H**, respectively, and compared with those of the parental BoHV-4-A isolate. The data the mean ± standard error of triplicate measurements ($P>0.05$ for all time-points; Student's *t*-test). The results of immunoblotting analyses conducted on extracts from cells infected with BoHV-4-RHuT-gD, BoHV-4-RRT-Fc and BoHV-4-RRT-gD are shown in panels **C**, **F** and **I**, respectively; BoHV-4-A infected cells served as negative controls.

Figure 5. Anti-Her-2-specific immune responses induced by intraperitoneal vaccination with the different recombinant BoHV-4 viral particles. (**A**) Sera from BALB/c mice (n=7), collected two weeks after the second vaccination , analyzed (at a 1:100 dilution) for the presence of specific anti-rat-HerR-2 antibodies by flow cytometry. Results are expressed as mean fluorescence intensity (MFI) values for each serum; horizontal lines represent median values (***: $p<0.0001$; Student's t-test). (**B**) *In*

vivo cytotoxic responses against the $H2^d$ dominant, rat Her-2 peptide TYVPANASL measured in mice immunized with the indicated BoHV-4 viral particles (n=3) two weeks after the second vaccination; data are mean ± SEM values (***: p=0.0004; Student's t-test. (**C**) T-cell responses against the $H2^d$ dominant, rat Her-2 TYVPANASL peptide determined two weeks after the second vaccination by an *in vitro* IFN-γ-based ELISPOT assay. IFN-γ-producing cells from mice immunized with the indicated BoHV-4 viral particles (n=3) are expressed as SFU/$1x10^6$ SPC; data are mean ± SEM values (***:, p<0.0001; Student's t-test).

Figure 6. Anti-rat-Her-2 antibody production and delayed mammary tumor appearance induced by vaccination with BoHV-4-RHuT-gD viral particles. (**A**) Sera from BALB-neuT mice, collected two weeks after the first (*grey dots*; n=8 to 17 animals/group) and the second (*black dots*; n=7-17 animals/group) i.p. immunization with the indicated BoHV-4 particles, were analyzed by flow cytometry (at a 1.100 dilution) for the presence of specific anti-rat-Her-2 antibodies. Results are expressed as mean fluorescence intensity (MFI) values for each serum; horizontal lines represent median values (***: p<0.0001; Student's t-test). (**B**) Mammary tumor incidence in control BoHV-4-A29-gD (*dotted gray line*, n=8), BoHV-4-RRT-gD, (*dotted black line*, n=11), BoHV-4-RRT-Fc (*solid black line*, n = 11) and BoHV-4-RHuT-gD (*solid red line*, n=17) BALB-neuT mice vaccinated with the indicated BoHV-4 viral particles (***: p<0.0001; Mantel-Haenszel Log-rank test).

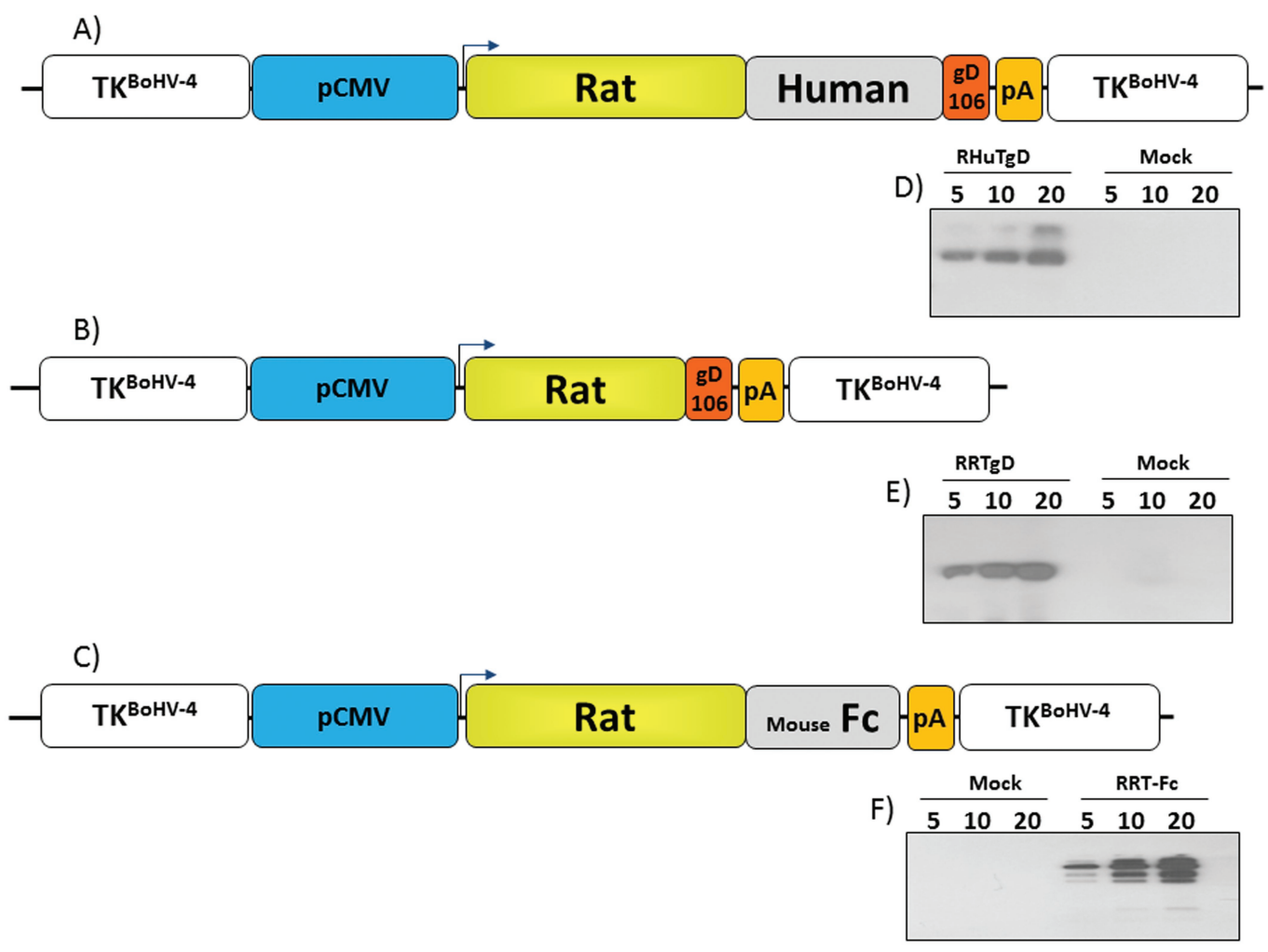
A)
TK BoHV-4
pCMV
Rat
Human
gD 106
pA
TK BoHV-4
D)
RHuTgD
Mock
5 10 20 5 10 20
B)
TK BoHV-4
pCMV
Rat
gD 106
pA
TK BoHV-4
E)
RRTgD
Mock
5 10 20 5 10 20
C)
TK BoHV-4
pCMV
Rat
Mouse Fc
pA
TK BoHV-4
F)
Mock
RRT-Fc
5 10 20 5 10 20

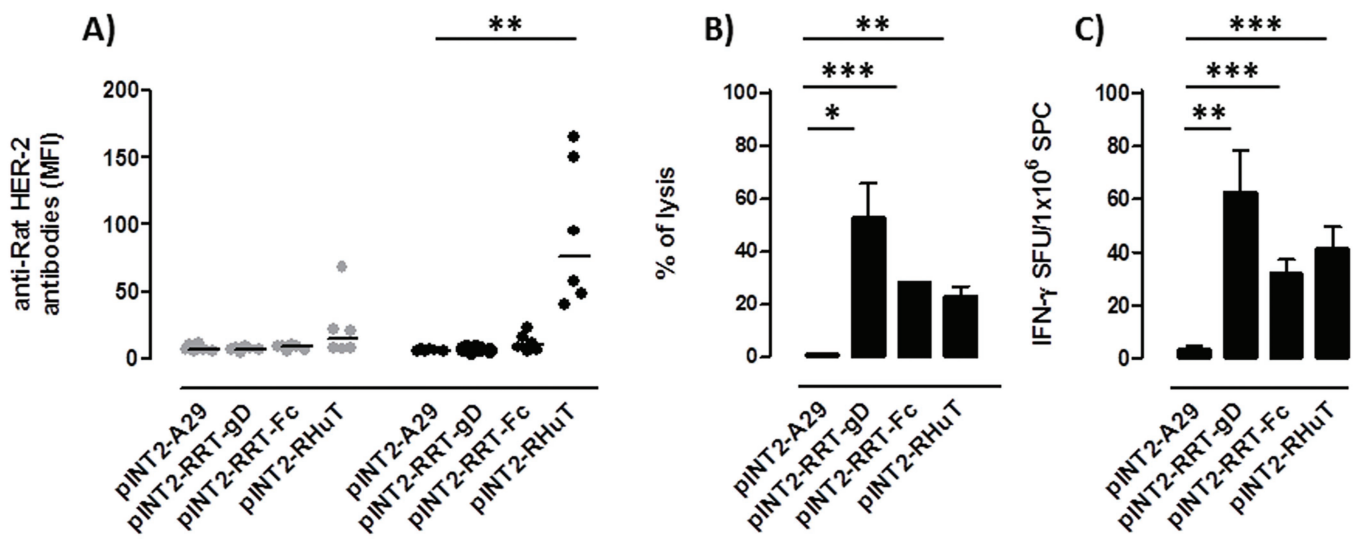
A)
**
200
150
100
50
0
anti-Rat HER-2 antibodies (MFI)
pINT2-A29
pINT2-RRT-gD
pINT2-RRT-Fc
pINT2-RHuT
pINT2-A29
pINT2-RRT-gD
pINT2-RRT-Fc
pINT2-RHuT
B)
**
***
*
100
80
60
40
20
0
% of lysis
pINT2-A29
pINT2-RRT-gD
pINT2-RRT-Fc
pINT2-RHuT
C)
***
***
**
100
80
60
40
20
0
IFN-γ SFU/1x10^6 SPC
pINT2-A29
pINT2-RRT-gD
pINT2-RRT-Fc
pINT2-RHuT

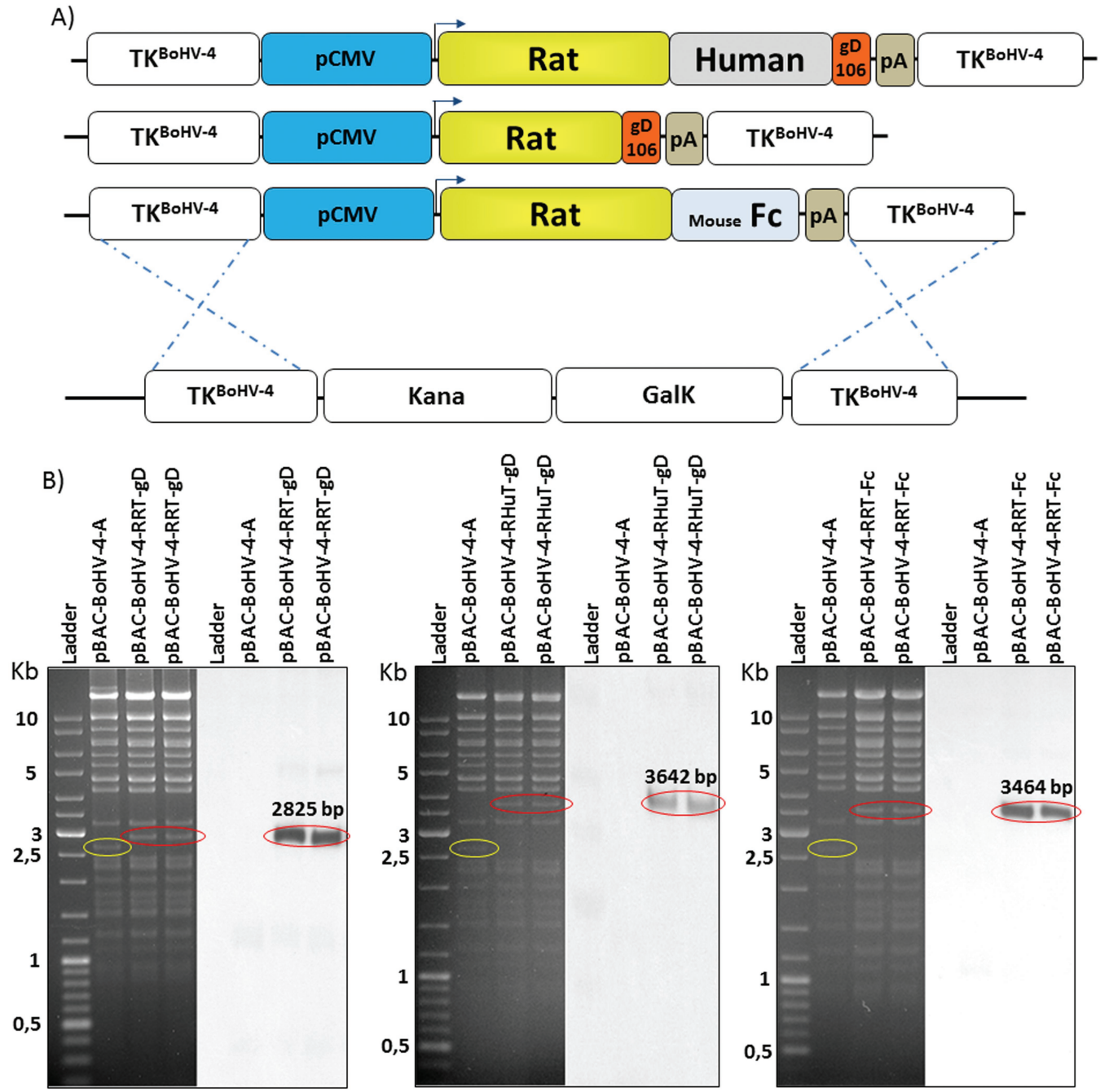
A)
TK BoHV-4
pCMV
Rat
Human
gD 106
pA
TK BoHV-4
TK BoHV-4
pCMV
Rat
gD 106
pA
TK BoHV-4
TK BoHV-4
pCMV
Rat
Mouse Fc
pA
TK BoHV-4
TK BoHV-4
Kana
GalK
TK BoHV-4
B)
Ladder
pBAC-BoHV-4-A
pBAC-BoHV-4-RRT-gD
pBAC-BoHV-4-RRT-gD
Ladder
pBAC-BoHV-4-A
pBAC-BoHV-4-RRT-gD
pBAC-BoHV-4-RRT-gD
Kb
10
5
3
2,5
1
0,5
2825 bp
Ladder
pBAC-BoHV-4-A
pBAC-BoHV-4-RHuT-gD
pBAC-BoHV-4-RHuT-gD
Ladder
pBAC-BoHV-4-A
pBAC-BoHV-4-RHuT-gD
pBAC-BoHV-4-RHuT-gD
Kb
10
5
3
2,5
1
0,5
3642 bp
Ladder
pBAC-BoHV-4-A
pBAC-BoHV-4-RRT-Fc
pBAC-BoHV-4-RRT-Fc
Ladder
pBAC-BoHV-4-A
pBAC-BoHV-4-RRT-Fc
pBAC-BoHV-4-RRT-Fc
Kb
10
5
3
2,5
1
0,5
3464 bp

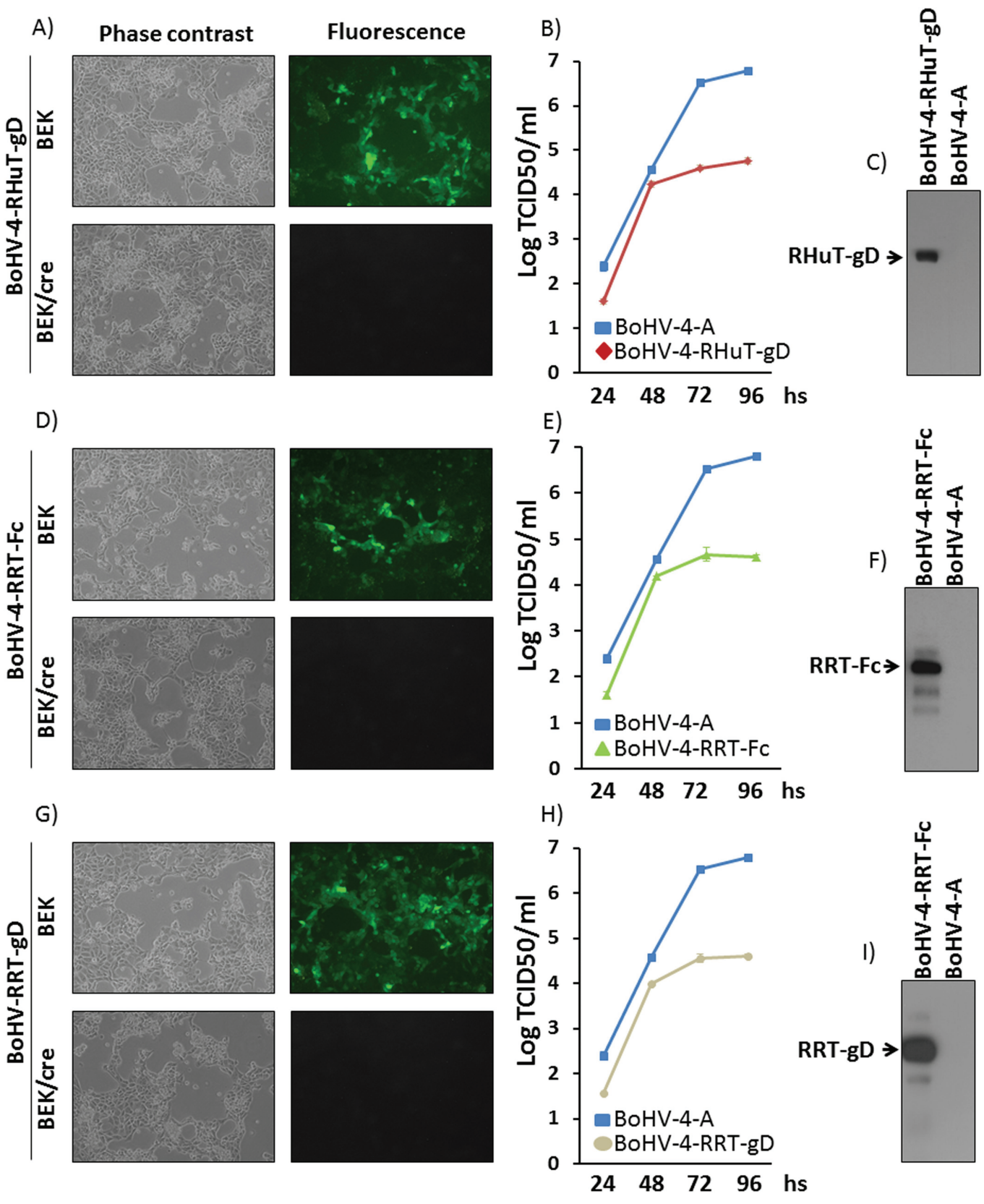
A)
Phase contrast
Fluorescence
BoHV-4-RHuT-gD
BEK
BEK/cre
B)
Log TCID50/ml
BoHV-4-A
BoHV-4-RHuT-gD
24 48 72 96 hs
C)
BoHV-4-RHuT-gD
BoHV-4-A
RHuT-gD
D)
BoHV-4-RRT-Fc
BEK
BEK/cre
E)
Log TCID50/ml
BoHV-4-A
BoHV-4-RRT-Fc
24 48 72 96 hs
F)
BoHV-4-RRT-Fc
BoHV-4-A
RRT-Fc
G)
BoHV-RRT-gD
BEK
BEK/cre
H)
Log TCID50/ml
BoHV-4-A
BoHV-4-RRT-gD
24 48 72 96 hs
I)
BoHV-4-RRT-Fc
BoHV-4-A
RRT-gD

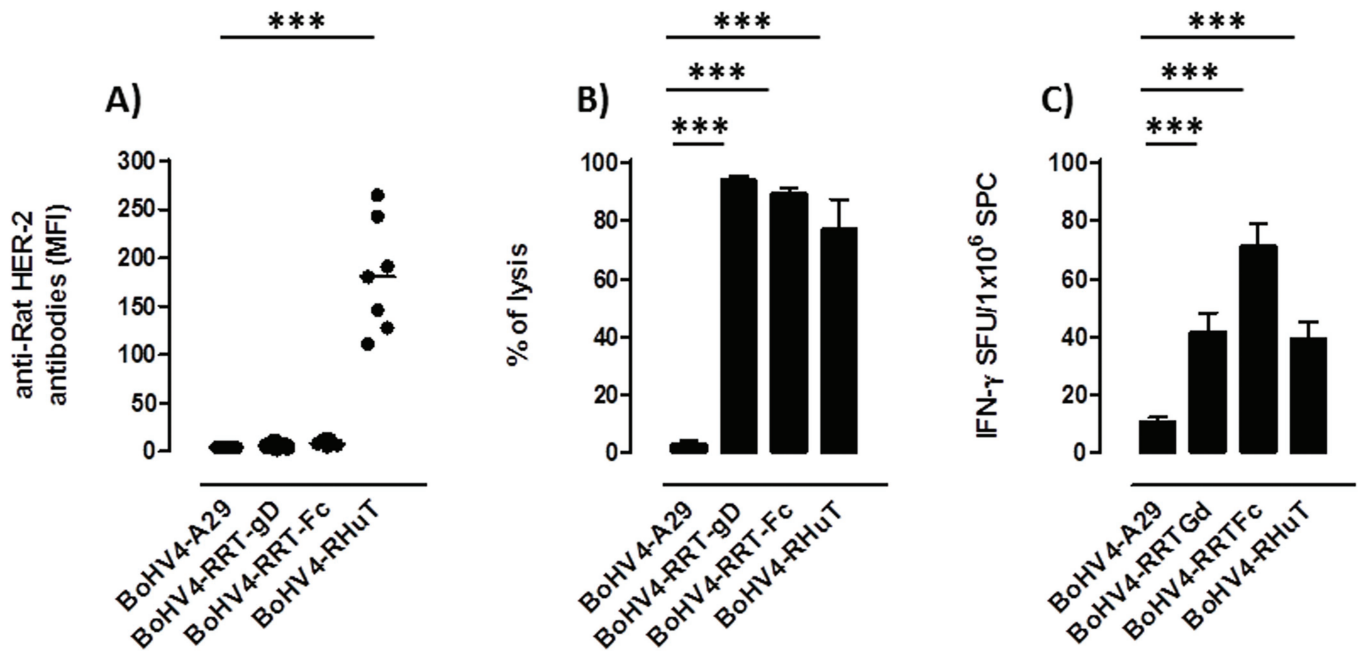
A)
B)
C)
***
anti-Rat HER-2 antibodies (MFI)
% of lysis
IFN-γ SFU/1x10^6 SPC
300
250
200
150
100
50
0
100
80
60
40
20
0
BoHV4-A29
BoHV4-RRT-gD
BoHV4-RRT-Fc
BoHV4-RHuT
BoHV4-RRTGd
BoHV4-RRTFc

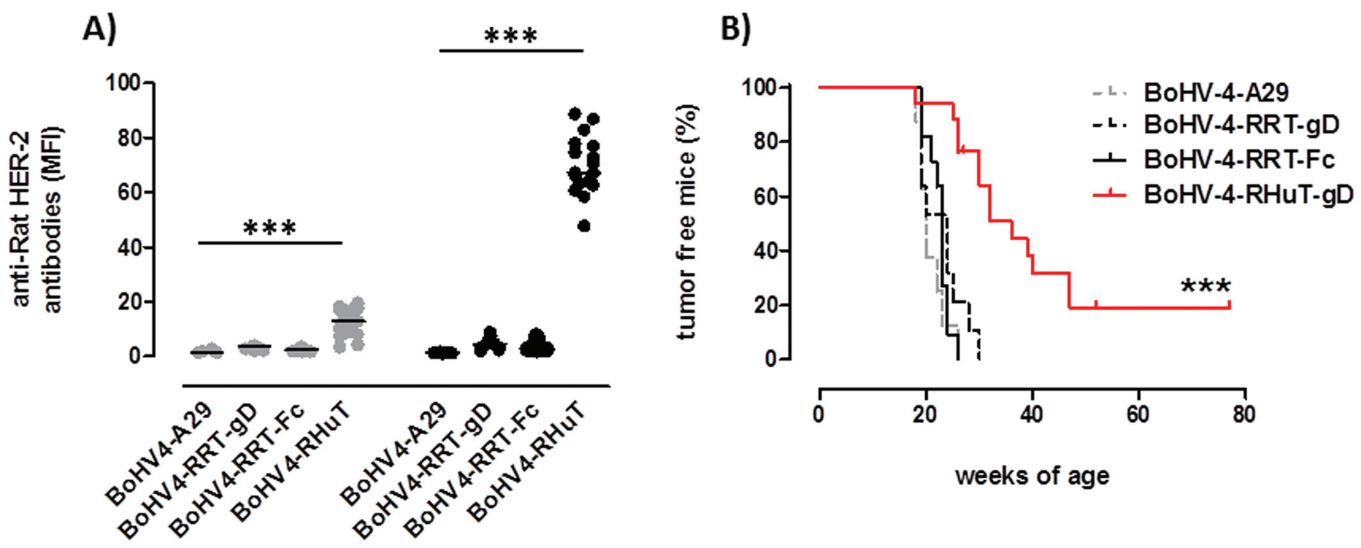
A)
anti-Rat HER-2 antibodies (MFI)
100
80
60
40
20
0
***
***
BoHV4-A29
BoHV4-RRT-gD
BoHV4-RRT-Fc
BoHV4-RHuT
BoHV4-A29
BoHV4-RRT-gD
BoHV4-RRT-Fc
BoHV4-RHuT
B)
tumor free mice (%)
100
80
60
40
20
0
BoHV-4-A29
BoHV-4-RRT-gD
BoHV-4-RRT-Fc
BoHV-4-RHuT-gD
***
0
20
40
60
80
weeks of age

atgatcatcatggagctggcggcctggtgccgctgggggttcctcctcgccctcctgccc
M I I M E L A A W C R W G F L L A L L P
cccggaatcgcgggcacccaagtgtgtaccggcacagacatgaagttgcggctccctgcc
P G I A G T Q V C T G T D M K L R L P A
agtcctgagacccacctggacatgctccgccacctgtaccagggctgtcaggtagtgcag
S P E T H L D M L R H L Y Q G C Q V V Q
ggcaacttggagcttacctacgtgcctgccaatgccagcctctcattcctgcaggacatc
G N L E L T Y V P A N A S L S F L Q D I
caggaagttcagggttacatgctcatcgctcacaaccaggtgaagcgcgtcccactgcaa
Q E V Q G Y M L I A H N Q V K R V P L Q
aggctgcgcatcgtgagagggacccagctctttgaggacaagtatgccctggctgtgcta
R L R I V R G T Q L F E D K Y A L A V L
gacaaccgagatcctcaggacaatgtcgccgcctccaccccaggcagaaccccagagggg
D N R D P Q D N V A A S T P G R T P E G
ctgcgggagctgcagcttcgaagtctcacagagatcctgaagggaggagttttgatccgt
L R E L Q L R S L T E I L K G G V L I R
gggaaccctcagctctgctaccaggacatggttttgtggaaggacgtcttccgcaagaat
G N P Q L C Y Q D M V L W K D V F R K N
aaccaactggctcctgtcgatatagacaccaatcgttcccgggcctgtccaccttgtgcc
N Q L A P V D I D T N R S R A C P P C A
cccgcctgcaaagacaatcactgttggggtgagagtccggaagactgtcagatcttgact
P A C K D N H C W G E S P E D C Q I L T
ggcaccatctgtaccagtggttgtgcccggtgcaagggccggctgcccactgactgctgc
G T I C T S G C A R C K G R L P T D C C
catgagcagtgtgccgcaggctgcacgggccccaagcattctgactgcctggcctgcctc
H E Q C A A G C T G P K H S D C L A C L
cacttcaatcatagtggtatctgtgagctgcactgcccagccctcgtcacctacaacaca
H F N H S G I C E L H C P A L V T Y N T
gacacctttgagtccatgcacaaccctgagggtcgctacacctttggtgccagctgcgtg
D T F E S M H N P E G R Y T F G A S C V
accacctgcccctacaactacctgtctacggaagtgggatcctgcactctggtgtgtccc
T T C P Y N Y L S T E V G S C T L V C P
ccgaataaccaagaggtcacagctgaggacggaacacagcgttgtgagaaatgcagcaag
P N N Q E V T A E D G T Q R C E K C S K
ccctgtgctcgagtgtgctatggtctgggcatggagcaccttcgaggggcgagggccatc
P C A R V C Y G L G M E H L R G A R A I
accagtgacaatgtccaggagtttgatggctgcaagaagatctttgggagcctggcattt
T S D N V Q E F D G C K K I F G S L A F
ttgccggagagctttgatggggacccctcctccggcattgctccgctgaggcctgagcag
L P E S F D G D P S S G I A P L R P E Q
ctccaagtgttcgaaaccctggaggagatcacaggttacctatacatctcagcatggccg
L Q V F E T L E E I T G Y L Y I S A W P
gacagcctgcctgacctcagcgtcttccagaacctgcaagtaatccggggacgaattctg
D S L P D L S V F Q N L Q V I R G R I L
cacaatggcgcctactcgctgaccctgcaagggctgggcatcagctggctggggctgcgc
H N G A Y S L T L Q G L G I S W L G L R
tcactgagggaactgggcagtggactggccctcatccaccataacacccacctctgcttc
S L R E L G S G L A L I H H N T H L C F
gtgcacacggtgccctgggaccagctctttcggaacccgcaccaagctctgctccacact
V H T V P W D Q L F R N P H Q A L L H T
gccaaccggccagaggacgagtgtgtgggcgagggcctggcctgccaccagctgtgcgcc
A N R P E D E C V G E G L A C H Q L C A
cgagggcactgctggggtccagggcccacccagtgtgtcaactgcagccagttccttcgg
R G H C W G P G P T Q C V N C S Q F L R
ggccaggagtgcgtggaggaatgccgagtactgcaggggctccccagggagtatgtgaat
G Q E C V E E C R V L Q G L P R E Y V N
gccaggcactgtttgccgtgccaccctgagtgtcagccccagaatggctcagtgacctgt
A R H C L P C H P E C Q P Q N G S V T C
tttggaccggaggctgaccagtgtgtggcctgtgcccactataaggaccctcccttctgc
F G P E A D Q C V A C A H Y K D P P F C
gtggcccgctgccccagcggtgtgaaacctgacctctcctacatgcccatctggaagttt
V A R C P S G V K P D L S Y M P I W K F
ccagatgaggagggcgcatgccagccttgccccatcaactgcacccactcctgtgtggac
P D E E G A C Q P C P I N C T H S C V D
ctggatgacaagggctgccccgccgagcagagagccagccctctgacgtccatcgtctct
L D D K G C P A E Q R A S P L T S I V S
gcggtggttggcattctgctggtcgtggtcttgggggtggtctttgggatcctcatcaag
A V V G I L L V V V L G V V F G I L I K
cgacggcagcagaagatccggaaggtcgactactggttcatgcgccacgggggcgtcgtt
R R Q Q K I R K V D Y W F M R H G G V V
ccgccgtattttgaggagtcgaagggctacgagccgccgcctgccgccgatgggggttcc
P P Y F E E S K G Y E P P P A A D G G S
ccctaa
P –

Supplementary Figure 1. Diagram (not to scale), nucleotide and deduced polypeptide sequence of the RHuT-gD chimeric protein/ORF. The rat and the human portions are highlighted in *yellow* and *grey*, respectively; the gD106 tag is highlighted in *red*.


```
atgatcatcatggagctggcggcctggtgccgctgggggttcctcctcgccctcctgccc
 M  I  I  M  E  L  A  A  W  C  R  W  G  F  L  L  A  L  L  P
cccggaatcgcgggcacccaagtgtgtaccggcacagacatgaagttgcggctccctgcc
 P  G  I  A  G  T  Q  V  C  T  G  T  D  M  K  L  R  L  P  A
agtcctgagacccacctggacatgctccgccacctgtaccagggctgtcaggtagtgcag
 S  P  E  T  H  L  D  M  L  R  H  L  Y  Q  G  C  Q  V  V  Q
ggcaacttggagcttacctacgtgcctgccaatgccagcctctcattcctgcaggacatc
 G  N  L  E  L  T  Y  V  P  A  N  A  S  L  S  F  L  Q  D  I
caggaagttcagggttacatgctcatcgctcacaaccaggtgaagcgcgtcccactgcaa
 Q  E  V  Q  G  Y  M  L  I  A  H  N  Q  V  K  R  V  P  L  Q
aggctgcgcatcgtgagagggacccagctctttgaggacaagtatgccctggctgtgcta
 R  L  R  I  V  R  G  T  Q  L  F  E  D  K  Y  A  L  A  V  L
gacaaccgagatcctcaggacaatgtcgccgcctccaccccaggcagaaccccagagggg
 D  N  R  D  P  Q  D  N  V  A  A  S  T  P  G  R  T  P  E  G
ctgcgggagctgcagcttcgaagtctcacagagatcctgaagggaggagttttgatccgt
 L  R  E  L  Q  L  R  S  L  T  E  I  L  K  G  G  V  L  I  R
gggaaccctcagctctgctaccaggacatggttttgtggaaggacgtcttccgcaagaat
 G  N  P  Q  L  C  Y  Q  D  M  V  L  W  K  D  V  F  R  K  N
aaccaactggctcctgtcgatatagacaccaatcgttcccgggcctgtccaccttgtgcc
 N  Q  L  A  P  V  D  I  D  T  N  R  S  R  A  C  P  P  C  A
cccgcctgcaaagacaatcactgttggggtgagagtccggaagactgtcagatcttgact
 P  A  C  K  D  N  H  C  W  G  E  S  P  E  D  C  Q  I  L  T
ggcaccatctgtaccagtggttgtgcccggtgcaagggccggctgcccactgactgctgc
 G  T  I  C  T  S  G  C  A  R  C  K  G  R  L  P  T  D  C  C
catgagcagtgtgccgcaggctgcacgggccccaagcattctgactgcctggcctgcctc
 H  E  Q  C  A  A  G  C  T  G  P  K  H  S  D  C  L  A  C  L
cacttcaatcatagtggtatctgtgagctgcactgcccagccctcgtcacctacaacaca
 H  F  N  H  S  G  I  C  E  L  H  C  P  A  L  V  T  Y  N  T
gacacctttgagtccatgcacaaccctgagggtcgctacacctttggtgccagctgcgtg
 D  T  F  E  S  M  H  N  P  E  G  R  Y  T  F  G  A  S  C  V
accacctgcccctacaactacctgtctacggaagtgggatcctgcactctggtgtgtccc
 T  T  C  P  Y  N  Y  L  S  T  E  V  G  S  C  T  L  V  C  P
ccgaataaccaagaggtcacagctgaggacggaacacagcgttgtgagaaatgcagcaag
 P  N  N  Q  E  V  T  A  E  D  G  T  Q  R  C  E  K  C  S  K
ccctgtgctcgagtgtgctatggtctgggcatggagcaccttcgaggggcgagggccatc
 P  C  A  R  V  C  Y  G  L  G  M  E  H  L  R  G  A  R  A  I
accagtgacaatgtccaggagtttgatggctgcaagaagatctttgggagcctggcattt
 T  S  D  N  V  Q  E  F  D  G  C  K  K  I  F  G  S  L  A  F
ttgccggagagctttgatggggacccctcctccggcattgctccgctgaggcctgagcag
 L  P  E  S  F  D  G  D  P  S  S  G  I  A  P  L  R  P  E  Q
ctccaagtgttcgaaaccctggaggagatcacagtcgactactggttcatgcgccacggg
 L  Q  V  F  E  T  L  E  E  I  T  V  D  Y  W  F  M  R  H  G
ggcgtcgttccgccgtattttgaggagtcgaagggctacgagccgccgcctgccgccgat
 G  V  V  P  P  Y  F  E  E  S  K  G  Y  E  P  P  P  A  A  D
gggggttccccctaa
 G  G  S  P  -
```

Supplementary Figure 2. Diagram (not to scale), nucleotide and deduced polypeptide sequence of the RRT-gD chimeric protein/ORF. The rat HER-2 and the gD106 tag portions are highlighted in *yellow* and *red*, respectively.


```
atgatcatcatggagctggcggcctggtgccgctgggggttcctcctcgccctcctgccc
 M  I  I  M  E  L  A  A  W  C  R  W  G  F  L  L  A  L  L  P
cccggaatcgcgggcacccaagtgtgtaccggcacagacatgaagttgcggctccctgcc
 P  G  I  A  G  T  Q  V  C  T  G  T  D  M  K  L  R  L  P  A
agtcctgagacccacctggacatgctccgccacctgtaccagggctgtcaggtagtgcag
 S  P  E  T  H  L  D  M  L  R  H  L  Y  Q  G  C  Q  V  V  Q
ggcaacttggagcttacctacgtgcctgccaatgccagcctctcattcctgcaggacatc
 G  N  L  E  L  T  Y  V  P  A  N  A  S  L  S  F  L  Q  D  I
caggaagttcagggttacatgctcatcgctcacaaccaggtgaagcgcgtcccactgcaa
 Q  E  V  Q  G  Y  M  L  I  A  H  N  Q  V  K  R  V  P  L  Q
aggctgcgcatcgtgagagggacccagctctttgaggacaagtatgccctggctgtgcta
 R  L  R  I  V  R  G  T  Q  L  F  E  D  K  Y  A  L  A  V  L
gacaaccgagatcctcaggacaatgtcgccgcctccaccccaggcagaaccccagagggg
 D  N  R  D  P  Q  D  N  V  A  A  S  T  P  G  R  T  P  E  G
ctgcgggagctgcagcttcgaagtctcacagagatcctgaagggaggagttttgatccgt
 L  R  E  L  Q  L  R  S  L  T  E  I  L  K  G  G  V  L  I  R
gggaaccctcagctctgctaccaggacatggttttgtggaaggacgtcttccgcaagaat
 G  N  P  Q  L  C  Y  Q  D  M  V  L  W  K  D  V  F  R  K  N
aaccaactggctcctgtcgatatagacaccaatcgttcccgggcctgtccaccttgtgcc
 N  Q  L  A  P  V  D  I  D  T  N  R  S  R  A  C  P  P  C  A
cccgcctgcaaagacaatcactgttggggtgagagtccggaagactgtcagatcttgact
 P  A  C  K  D  N  H  C  W  G  E  S  P  E  D  C  Q  I  L  T
ggcaccatctgtaccagtggttgtgcccggtgcaagggccggctgcccactgactgctgc
 G  T  I  C  T  S  G  C  A  R  C  K  G  R  L  P  T  D  C  C
catgagcagtgtgccgcaggctgcacgggccccaagcattctgactgcctggcctgcctc
 H  E  Q  C  A  A  G  C  T  G  P  K  H  S  D  C  L  A  C  L
cacttcaatcatagtggtatctgtgagctgcactgcccagccctcgtcacctacaacaca
 H  F  N  H  S  G  I  C  E  L  H  C  P  A  L  V  T  Y  N  T
gacacctttgagtccatgcacaaccctgagggtcgctacacctttggtgccagctgcgtg
 D  T  F  E  S  M  H  N  P  E  G  R  Y  T  F  G  A  S  C  V
accacctgcccctacaactacctgtctacggaagtgggatcctgcactctggtgtgtccc
 T  T  C  P  Y  N  Y  L  S  T  E  V  G  S  C  T  L  V  C  P
ccgaataaccaagaggtcacagctgaggacggaacacagcgttgtgagaaatgcagcaag
 P  N  N  Q  E  V  T  A  E  D  G  T  Q  R  C  E  K  C  S  K
ccctgtgctcgagtgtgctatggtctgggcatggagcaccttcgaggggcgagggccatc
 P  C  A  R  V  C  Y  G  L  G  M  E  H  L  R  G  A  R  A  I
accagtgacaatgtccaggagtttgatggctgcaagaagatctttgggagcctggcattt
 T  S  D  N  V  Q  E  F  D  G  C  K  K  I  F  G  S  L  A  F
ttgccggagagctttgatggggacccctcctccggcattgctccgctgaggcctgagcag
 L  P  E  S  F  D  G  D  P  S  S  G  I  A  P  L  R  P  E  Q
ctccaagtgttcgaaaccctggaggagatcacagtcgaccgtacgcggccgctcgagccc
 L  Q  V  F  E  T  L  E  E  I  T  V  D  R  T  R  P  L  E  P
agagggcccacaatcaagccctgtcctccatgcaaatgcccagcacctaacctcttgggt
 R  G  P  T  I  K  P  C  P  P  C  K  C  P  A  P  N  L  L  G
ggaccatccgtcttcatcttccctccaaagatcaaggatgtactcatgatctccctgagc
 G  P  S  V  F  I  F  P  P  K  I  K  D  V  L  M  I  S  L  S
cccatagtcacatgtgtggtggtggatgtgagcgaggatgacccagatgtccagatcagc
 P  I  V  T  C  V  V  V  D  V  S  E  D  D  P  D  V  Q  I  S
tggtttgtgaacaacgtggaagtacacacagctcagacacaaacccatagagaggattac
 W  F  V  N  N  V  E  V  H  T  A  Q  T  Q  T  H  R  E  D  Y
aacagtactctccgggtggtcagtgccctccccatccagcaccaggactggatgagtggc
 N  S  T  L  R  V  V  S  A  L  P  I  Q  H  Q  D  W  M  S  G
aaggagttcaaatgcaaggtcaacaacaaagacctcccagcgcccatcgagagaaccatc
 K  E  F  K  C  K  V  N  N  K  D  L  P  A  P  I  E  R  T  I
tcaaaacccaaagggtcagtaagagctccacaggtatatgtcttgcctccaccagaagaa
 S  K  P  K  G  S  V  R  A  P  Q  V  Y  V  L  P  P  P  E  E
gagatgactaagaaacaggtcactctgacctgcatggtcacagacttcatgcctgaagac
 E  M  T  K  K  Q  V  T  L  T  C  M  V  T  D  F  M  P  E  D
atttacgtggagtggaccaacaacgggaaaacagagctaaactacaagaacactgaacca
 I  Y  V  E  W  T  N  N  G  K  T  E  L  N  Y  K  N  T  E  P
gtcctggactctgatggttcttacttcatgtacagcaagctgagagtggaaaagaagaac
 V  L  D  S  D  G  S  Y  F  M  Y  S  K  L  R  V  E  K  K  N
tgggtggaaagaaatagctactcctgttcagtggtccacgagggtctgcacaatcaccac
 W  V  E  R  N  S  Y  S  C  S  V  V  H  E  G  L  H  N  H  H
acgactaagagcttctcccggactccgggtaaatga
 T  T  K  S  F  S  R  T  P  G  K  -
```

Supplementary Figure 3. Diagram (not to scale), nucleotide and deduced polypeptide sequence of the RRT-Fc chimeric protein/ORF. The rat HER-2 and the Fc portions are highlighted in *yellow* and *grey*, respectively.

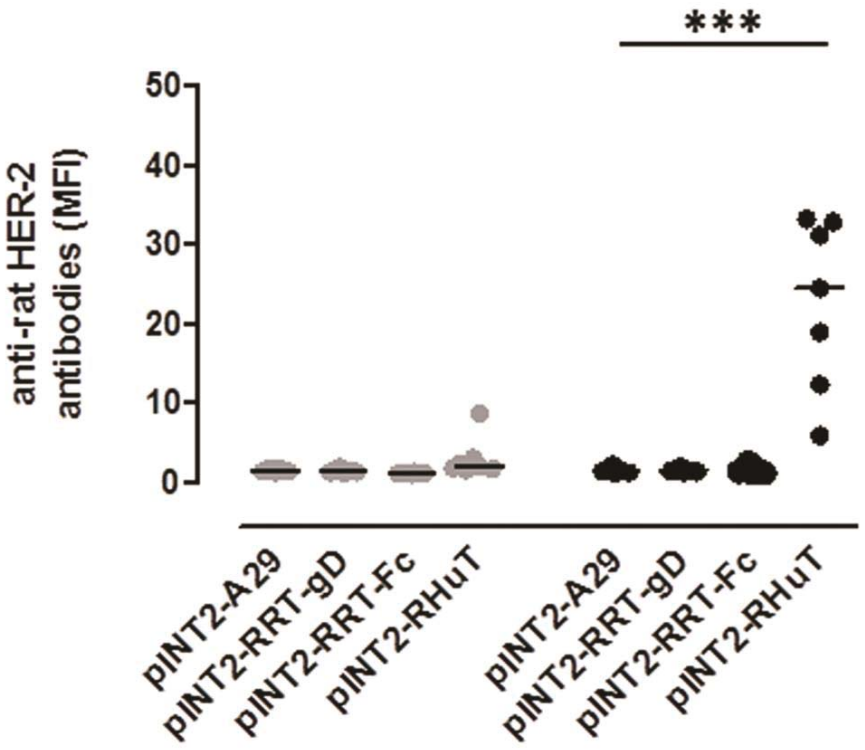

Supplementary Figure 4. Anti-rat-Her-2-specific antibodies elicited by i.p. vaccination of rat-HER-2-tolerant mice with the indicated recombinant pINT2 plasmids. Sera from BALB-neuT mice (n=7), collected two weeks after the first (*grey dots*) and the second (*black dots*) vaccination, were analyzed (at a 1:100 dilution) for the presence of specific anti-rat-Her-2 antibodies by flow cytometry. Results are expressed as mean fluorescence intensity (MFI) values for each serum; horizontal lines represent median values (***: p=0.0002; Student's t-test).

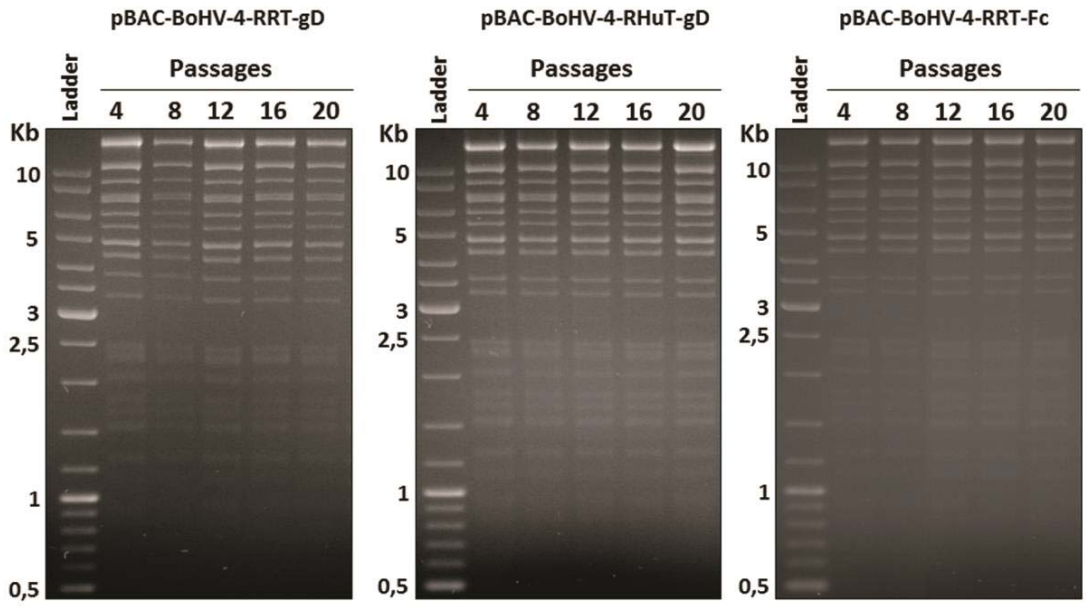

Supplementary Figure 5. Stability of the pBAC-BoHV-4-RHuT-gD, pBAC-BoHV-4-RRT-gD and pBAC-BoHV-4-RRT-gD plasmids after multiple passages (up to 20) in *E. coli* SW102 cells.

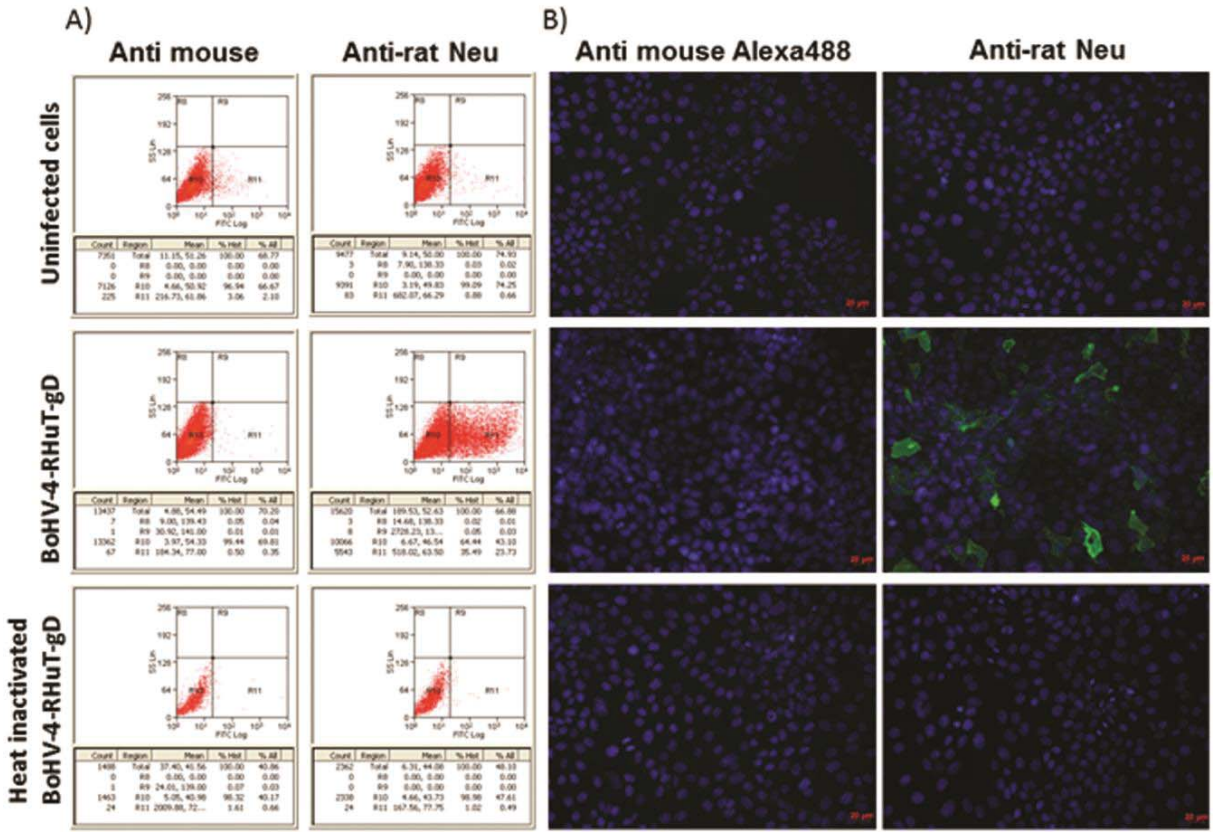

Supplementary figure 6. RHuT expressed on the cell surface of BoHV-4-RHuT-gD infected murine mammary epithelial cells is recognized by an anti rat-Her-2 monoclonal antibody**.** Cytofluorimetric (**A**) and immunofluorescence (**B**) staining of Nmug cells 24 hours after live (middle panels) and heat inactivated (lower panels) BoHV-4-RHuT-gD infection.